ISTANBUL TECHNICAL UNIVERSITY ★ GRADUATE SCHOOL OF SCIENCE ENGINEERING AND TECHNOLOGY

INVESTIGATION OF FLOW FIELD AROUND/THROUGH SIMPLIFIED EMERGENT ISOLATED TREE-LIKE VEGETATION

M.Sc. THESIS

Dorukhan KELLECİOĞLU

Department of Civil Engineering

Hydraulic and Water Resources Engineering Programme

Thesis Advisor: Assoc. Prof. Oral YAĞCI

JANUARY 2016

ISTANBUL TECHNICAL UNIVERSITY ★ GRADUATE SCHOOL OF SCIENCE ENGINEERING AND TECHNOLOGY

INVESTIGATION OF FLOW FIELD AROUND/THROUGH SIMPLIFIED EMERGENT ISOLATED TREE-LIKE VEGETATION

M.Sc. THESIS

Dorukhan KELLECİOĞLU
(501131505)

Department of Civil Engineering

Hydraulic and Water Resources Engineering Programme

Thesis Advisor: Assoc. Prof. Oral YAĞCI

JANUARY 2016

İSTANBUL TEKNİK ÜNİVERSİTESİ ★ FEN BİLİMLERİ ENSTİTÜSÜ

AKIMA BATMAMIŞ BASİTLEŞTİRİLMİŞ AĞAÇSI TEKİL BİTKİ CİVARINDAKİ AKIM ALANININ İNCELENMESİ

YÜKSEK LİSANS TEZİ

Dorukhan KELLECİOĞLU
(501131505)

İnşaat Mühendisliği Anabilim Dalı

Hidrolik ve Su Kaynakları Mühendisliği Programı

Tez Danışmanı: Doç. Dr. Oral YAĞCI

OCAK 2016

Dorukhan Kellecioğlu, a **M.Sc.** student of ITU **Graduate School of Science Engineering and Technology** student ID **501131505**, successfully defended the **thesis** entitled "**Investigation of Flow Field Around Simplified Emergent Isolated Tree-like Vegetation**", which he prepared after fulfilling the requirements specified in the associated legislations, before the jury whose signatures are below.

Thesis Advisor :	**Assoc. Prof. Dr. Oral YAĞCI** İstanbul Technical University	.....
Jury Members :	**Prof. Dr. Yalçın YÜKSEL** Yıldız Technical University	.....
	Prof. Dr. Hafzullah AKSOY İstanbul Technical University	.....

Date of Submission : 27 November 2015
Date of Defense : 19 January 2016

To my lovely mother and father as towers of strength,

FOREWORD

This thesis is written during my Master of Science study at Istanbul Technical University in the dates between September 2013 and November 2015 with the motivation of to be a crumb of information on river restoration purposes and to be able to contribute the endless knowledge on ecohydraulics. River restoration programmes and ecohydraulic studies are substantial. If the humankind continue to exploit the water resources with his greedy approach, living on earth will not be sustainable because of the absence of water which is the primarily need for humanity and the other living creatures.

I would like to thank my supervisor Assoc. Prof. Dr. Oral Yağcı for helping me with a great perspective and giving me valuable advice and support when needed. My biggest motivation source was his humanist personality and his avoid dictating his ideas without discussion. Other important person, who supports to the creation of this thesis with his determined and helpful personality, is Dr. Vasileios Kitsikoudis who is a postdoctoral researcher in Istanbul Technical University. We had endless discussion with him and he gave me eye-opening advices during my experiments and my study. Besides, I would like to thank Prof. Dr. Hafzullah Aksoy and Assoc. Prof. Dr. Özgür Kırca for giving me the oppurtunity to work with them in a European Union funded project named "A Scientific Network for Earthquake, Landslide & Flood Hazard Prevention" during my study. It was a great advantage to work in an international academic environment and with such experienced academicians. I also would like to thank Mevlüt Uluçınar from Istanbul Technical University Hydraulics Laboratory for helping me a lot for my experiments, his contribution on my experiments incontrovertible.

Finally, I would like to give my special thanks to my mother and father. This study would not be possible without their ultimate confidence and emotional support.

November 2015

Dorukhan KELLECİOĞLU
(Civil Engineer)

TABLE OF CONTENTS

Page

ABBREVIATIONS

TKE	**:** Turbulence Kinetic Energy
App	**:** Appendix
ADV	**:** Acoustic Doppler Velocimeter
Re	**:** Reynolds Number

LIST OF FIGURES

Page

FLOW AROUND/THROUGH SIMPLIFIED EMERGENT ISOLATED TREE-LIKE VEGETATION

SUMMARY

Rivers are perfect balanced formations which have been being evolved for hundred thousands of years with the natural effects such as morphological and/or biological effects. This perfect balance of rivers and waterfront areas are excessively fragile against human activities. Nowadays, river ecosystems are faced with human-induced impacts in a while that, is significantly short compared to long-drown-out evolution period. In recent years, exchanging human based artificial impacts with natural arrangments by understanding the river ecosystem dynamics is becoming hot topic in the river management community. In this new field, aquatic and riparian vegetation impacts are incontrovertible. To apply an ecological, multi-functional and sustainable river restoration comprehending deeply the both aquatic and riparian vegetation's role is crucial. Aquatic and riparian vegetation have great impacts on river ecosystems as, those plants increase the bank stability, provide habitat for animals and invertebrates, improve the water quality, build pioneer landforms by trapping and stabilizing sediment, promote biodiversity, regulate water temperature. The main motivation of this thesi is to contribute to ecological river restoration knowledge.

In the present study the flow field alteration of tree-like vegetation that are widespread located in riparian zones, which represents the interface between land and river. The plant canopy was simplified by placing different configurations of cylindrical elements onto a wooden rod and testing them individually, on the porpose of idealizing the complex architecture of the canopy in natural vegetation. The tested configurations are a rigid cylinder and two hexagonal arrays of circular cylinders with equal overall diameter. The tested hexagonal array configurations identified as dense array and sparse array according to their solid volume fractions, $\emptyset = 0.335$ and $\emptyset = 0.132$, respectively. Experiments done firstly with uniform forms of the solid cylinder and the hexagonal arrays, then same experiments conducted with tree-like elements, which the same obstacles served as canopies, and real vegetation (*Cupressus macrocarpa*). If the uniform and tree-like cases are considered as two different experiment groups. Comparisons made for all experiment groups in itself and in between.

AKIMA BATMAMIŞ BASİTLEŞTİRİLMİŞ AĞAÇSI TEKİL BİTKİ CİVARINDAKİ AKIMIN İNCELENMESİ

ÖZET

Nehirler, yüzbinlerce yıl içerisinde morfolojik ve biyolojik etkiler altında evrimleşmiş, bu sayede bulundukları koşullar ile muhteşem bir denge sağlamış oluşumlardır. Fakat bu muhteşem denge yüzbinlerce yıllık evrim ile karşılaştırıldığında aniden ortaya çıkan insan etkilerine karşı oldukça kırılgandır. Kanal pürüzlülüğünün azaltılması için bitkilerin temizlenmesi, kanallama uygulamaları, taşkın duvarları ile taşkın yataklarının akarsu yataklarından ayrılması, akarsu yataklarının beton veya benzeri malzemelerle kaplanması, baraj uygulamaları, bent uygulamaları, bağlama uygulamaları insani etkilere örnek olarak verilebilir. Nehir ekosistemi dinamiklerini anlayarak, insan kaynaklı yapay etkilerin yerini doğal düzenlemelerle doldurma çabası son yıllarda yükselen bir eğilim olarak görülmektedir. Bahsedilen doğal düzenlemelerin en önemli bileşenlerinin başında ise nehir kıyısı bitkileri ve sucul bitkiler gelmektedir. Ekolojik, sürdürülebilir ve çok fonksiyonlu bir nehir düzenlemesi yapabilmek adına nehir kıyısı bitkilerinin ve sucul bitkilerin ekosistem içindeki rolünü kavramak olmazsa olmazdır. Bu bitkilerin, şev stabilitesini sağlaması, hayvanlar ve omurgasızlar için elverişli yaşam alanları oluşturması, askıdaki katı maddenin tutulmasına olanak sağlayarak öncül arazi yapılarını yaratması, su kalitesini arttırması, biyoçeşitliliği desteklemesi ve su sıcaklığını düzenlemesi gibi nehir ekosistemlerine çok önemli etkileri bulunmaktadır. Dünyada bir çok örneği görülen ve uygulamaların gittikçe artmaya başladığı ekolojik nehir düzenlemesi yaklaşımının ülkemizde neredeyse hiç uygulanmadığı görülmektedir. Söz konusu tezin ana motivasyonu ise daha önce bahsedilen ekolojik nehir düzenlemesi yaklaşımına bir katkı oluşturmaktır.

Bu çalışmada, taşkın yatağında yoğun olarak bulunan iri gövdeli ağaçsı nehir kıyısı bitkilerinin akım alanı üzerindeki etkileri incelenmiştir. Bu alanda otsu nehir yatağı bitkileri üzerinde bir çok çalışma bulunsa da literatürde sap ve gövde olmak üzere iki ayrı bölümden olan ağaçsı bitkiler üzerinde bir çalışma bulunmamaktadır. İri gövdeli ağaçsı bitkileri ele alıyor olmak kanopi altı akımların oluşmasıyla birlikte problemi iki boyutlu olmaktan çıkarıp üçüncü boyutta da inceleme yapma gereksinimini doğurmaktadır. Fakat doğal bitkilerle sürdürülebilir deney yapmak, deney süresi boyunca bitkinin zamanla formunun değişmesi sebebiyle mümkün olmamaktadır. Bu çalışma ile hedeflenen, doğal bitki benzeri yapay konfigürasyonlar yaratabilmek, bu şekilde deneylerde yapay konfigürasyon kullanılsa dahi doğal bitki benzeri bir akım ortamı oluşturabilmektir. Eğer bu hedefe ulaşılabilirse, doğal bitki etrafı akımlarının anlaşılması kolaylaşacak ve buna bağlı olarak geliştirilecek nehir düzenleme çözümlerinin sürdürülebilir olması sağlanacaktır. Bu amaçla geliştirilen sistemede doğal bitkilerdeki kanopinin karmaşık yapısını idealize etmek amacıyla, kanopi bölgesi farklı silindirik elemanlar kullanılarak basitleşirilmiş ve ayrı ayrı test edilmiştir. Teste tabi tutulan konfigürasyonlar, rijit silindir ve rijit silindirle aynı dış

çapa sahip olmak üzere porozite değerleri farklı olan iki adet hegazagonal silindirdir. Bahsedilen hegzagonal silindirler 16 cm çaplı çemberin merkezine bir ve bu çemberin içine oturtulmuş altıgenin köşelerine birer tane olmak üzere toplamda yedi adet tekil silindirden oluşturulmuştur. Bu hegzagonal silindilerde kullanılan tekil silindirlerin çapları değiştirilerek farklı iki adet düzenek oluşturulmuş, bunlar yoğun düzen ve seyrek düzen olarak tanımlanmıştır. Sırasıyla tekil silindir çapları $D = 3.5\,cm,\ D = 2.2\,cm$ olarak belirlenmiş olup, dolu hacim oranları $\emptyset = 0.335$ ve $\emptyset = 0.132$ hesaplanmıştır. Deneyler mevcut çalışmalarla karşılaştırma yapılabilmesi adına öncelikle elementlerin üniform(derinlik boyunca enkesit şekli değişmeyen) formları ile gerçekleştirilmiş, sonrasında ise aynı engellerin tabanına eklenen ve ağaçsı bitkinin gövdesini karakterize eden ahşap silindir yardımıyla gövde tasvir edilmiş ve gerçekte mevcut olan üç boyutlu akım ortamı yaratılmıştır. Ayrıca gerçek bitkilerle karşılaştırma yapabilek adına yine ortalama dış çapı $D = 16\,cm$ limoni servi (*Cupressus macrocarpa*) sucul bitkisi ile de aynı ölçümler yapılmıştır.

1. INTRODUCTION

Flow and wake structure around/through a porous obstruction, is an ongoing research subject on many engineering fields. Understanding the flow around a porous obstruction is important in many science contexts as pile groups, windbreakers, heat exchangers and aquatic and terrestrial vegetation (Munson et al., 2009). Mainly scope of this study is to contribute to the knowledge regarding the flow around/through aquatic and riparian vegetation. Aquatic and riparian vegetation have great impacts on river ecosystems as, increasing the bank stability, providing habitat for animals and invertebrates, improving the water quality, building pioneer landforms by trapping and stabilizing sediment, promoting biodiversity and regulating water temperature. (Gurnell A. , 2014)

1.1 Fundamental Background

Flow over immersed bodies has been one of the most important topics in the fluid dynamics for many years. There is no doubt that the character of the flow field changes depending on the shape of the body. Relatively simple geometric forms are expected to have less complex flow fields when flow passes around/through it. However, even simple obstacle geometries such as uniform solid cylinder can produce quite complex flow structures. In order to give a better insight to the problem some major theorems such as boundary layer hydrodynamic and turbulence are useful. From this motivation herein, some fundamental aspects, which may facilitate the interpretation of the results, are presented below.

1.1.1 Boundary layer

Boundary layer is the layer of fluid, which is in the immediate vicinity of a bounding surface where the effects of viscosity are significant. In boundary layer viscous effects dominates the flow field rather than the inertial effects. Generally, objects those have a characteristic length, l, on order of $0.01\ m < l < 10\ m$ are exposed to external flows that we are familiar. Besides, the common fluids are water or air and

their ordinary upstream velocities are on the order of $0.01\ m/s < l < 100\ m/s$. As result of these values, Reynolds number range for such fluids is in the neighborhood of $10 < Re < 10^9$ as shown in Figure 1.1. Flows with $Re > 100$ are dominated by inertial effects, however flows with $Re < 1$ are dominated by viscous effects. Thereby, most common external flows are dominated by inertia (Munson et al., 2009).

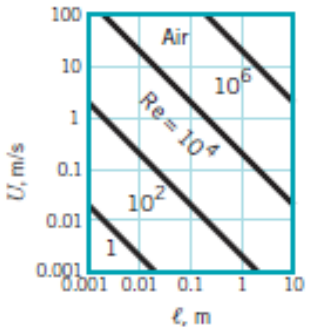

Figure 1.1 : Changing Reynolds number according to change in flow velocity and characteristic length of obstacle (Munson et al., 2009).

On the other hand, there are many external flows with Reynolds number considerably smaller than unity which means that viscous forces are more important than the inertial forces. For instance, low Reynolds number flow principles govern the gradual settling of small particles in lake or stream according to the small diameters and small settling speed. In addition, objects moving in large viscosity oils are governed by those principles because of large values of μ. Illustrations, which are drawn by considering flow past a streamlined and blunt object as a flat plate parallel to the upstream velocity and a circular cylinder, are adequate to show the general differences between low and high Reynolds number (Munson et al., 2009).

Flow pass three flat plates of length l with $Re = \rho U l/\mu = 0.1, 10$ and 10^7 are shown in Figure 1.2. In the condition which Reynolds number is small, the viscous effects are relatively dominant then inertia effects, and the plate disturbs the uniform upstream flow far ahead, above, below and behind the plate. To reach that undisturbed portion of flow that is indicated by where the velocity has been diminished by less than 1 % of the undisturbed value, a specific distance far from the plate is needed. In all directions, viscous effects are felt far from the object in the surrounding fluid in the case of low Reynolds number flow (Munson et al., 2009).

As is shown in Figure 1.2 when Reynolds number increased (for example by increasing U), the region which viscous effects important getting smaller in all directions. With increasing Reynolds number, streamline deflections become smaller because of the shrunken viscous region. If the Reynolds number is large, inertial effects dominate the flow. The viscous effects are negligibly small except in a very thin layer called viscous region around the plate and the relatively small wake region behind the plate. (White, 2001)

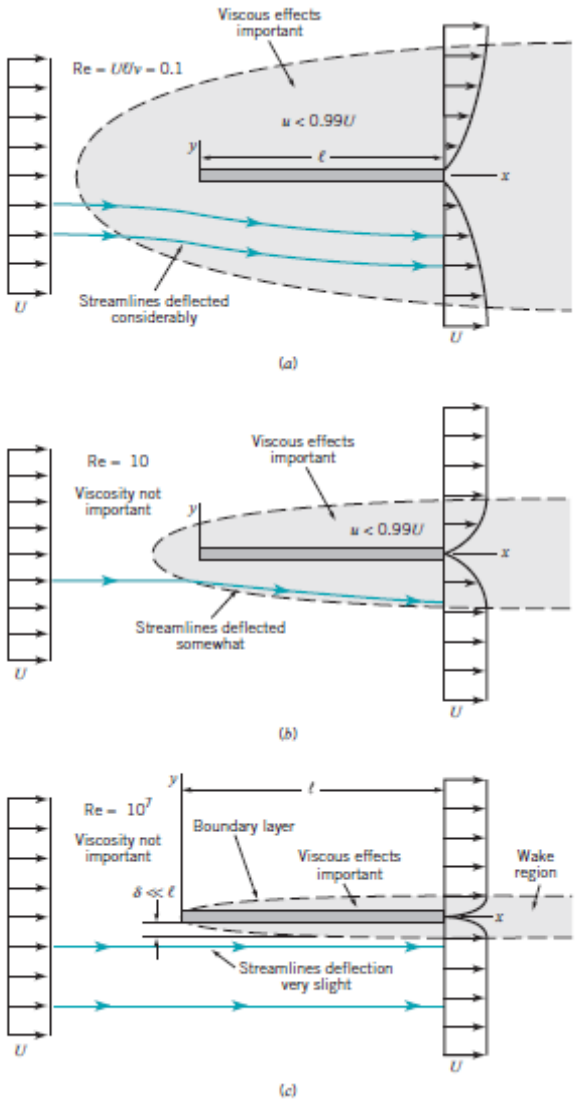

Figure 1.2 : Character of the steady, viscous flow past a flat plate parallel to the upstream velocity: (a) low Reynolds number flow, (b) moderate Reynolds number flow, (c) large Reynolds number flow (Munson et al., 2009).

Fluid must stick to the solid surface since fluid viscosity is not zero. Because of this sticked fluid, there is a boundary region that the flow velocity changes from zero to

the upstream value U. In the direction of flow, thickness of this layer typically increases along the plate.

It is a better approach to understand the boundary layer by focusing a fluid particle that moves into the boundary layer. As is indicated in Figure 1.3 while a rectangular particle flow in the uniform flow outside the boundary layer, it retains its rectangular form. After it enters the boundary layer, particle starts to distort because the presence of the velocity gradients in the viscous layer. The flow outside the boundary layer has zero vorticity as irrotational, inside the boundary layer as rotational flow. After a distance, the boundary layer flow becomes turbulent. Because of the unpredictable and irregular structure of the turbulence, fluid particles become enormously distorted.

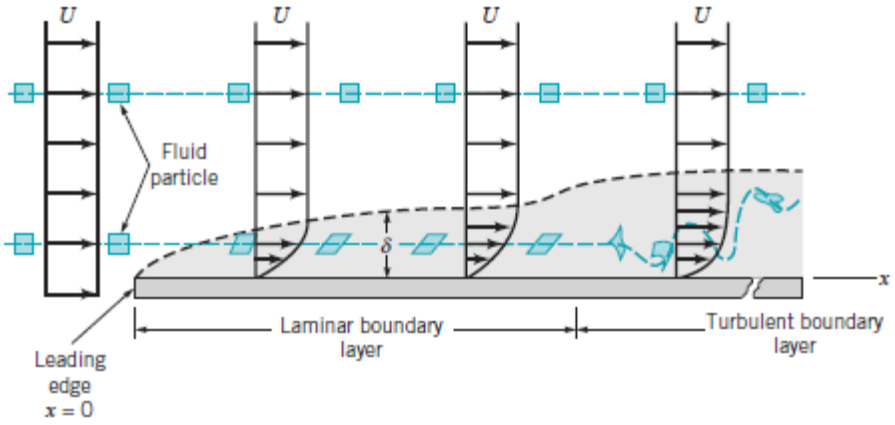

Figure 1.3 : Distortion of a fluid particle as it flows within the boundary layer (Munson et al., 2009).

1.1.2 Flow seperation

Reynolds number ($Re = UD/v < 1$) pass around a circular cylinder, relatively large portion of surrounding flow (several diameters from object) is dominated by viscous effects as indicated in Figure 1.4(a). Fundamentally, streamlines around the cylinder are symmetric about the center of the cylinder for low Reynolds number case.

Associated with the increasing Reynolds number, viscous region ahead the cylinder becomes smaller. The viscous effects are convected downstream and the flow loses its symmetry about the center of the cylinder. With this deformation, an important

characteristic of external flows become apparent called separation location as indicated in Figure 1.4(b).

Fluid inertia becomes more important with the increasing Reynolds number. At some point called separation location, fluid's inertia does not allow the fluid to follow the curved path about the rear of the blunt body. As a result, separation bubble occurs behind the body that the fluid is flowing upstream.

At larger Reynolds numbers, the area affected by viscous forces squash into a thin boundary layer on the front part of the cylinder. On the other hand, an irregular, unsteady wake region extends behind cylinder as indicated in Figure 1.4(c). In the

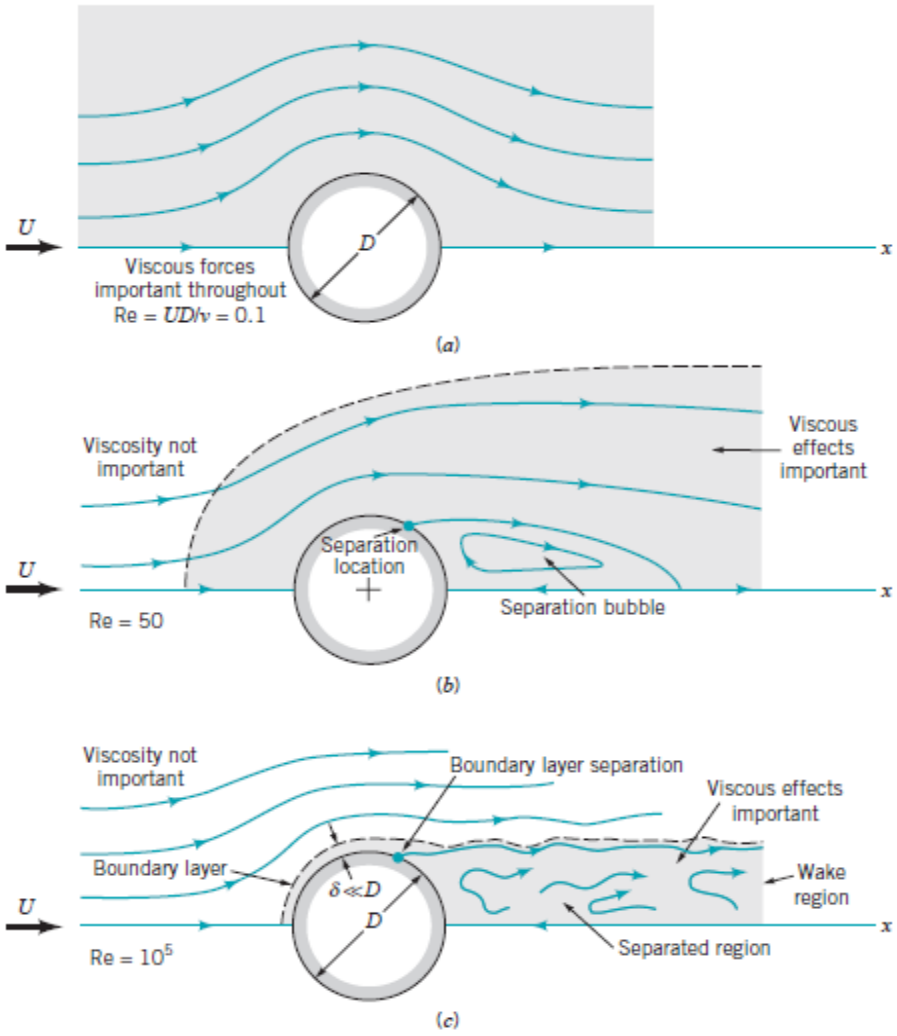

Figure 1.4 : Character of the steady, viscous flow past a circular cylinder: (*a*) low Reynolds number flow, (*b*) moderate Reynolds number flow, (*c*) large Reynolds number flow (Munson et al., 2009).

wake region or boundary layer, the velocity gradients are much larger than the remaining part of the flow, which the viscous affects are not important.

If these vortices exposed to the small disturbances they loose their stabilization easily. As consequence, if $Re > 40$ one vortex will grow larger than the other will. Thus "The larger vortex (Vortex A in Figure 1.5) presumably becomes strong enough to draw the opposing vortex (Vortex B) across the wake" (Sumer & Fredsoe, 2006, p. 9) as sketched in Figure 1.5. The vorticities of Vortex A and Vortex B are in the opposite directions which, vorticity of Vortex A is in clockwise direction and the other is in anti-clockwise direction. Because of this drawing effect, Vortex B approaches to Vortex A and opposite signed vortice blocks the supply of vorticity to Vortex A from its boundary layer. This is the exact moment that vortex A shed. After the shedding of Vortex A, a new vortex will develop at the same side of the obstacle, namely Vortex C. Now Vortex B will undertake the role of Vortex A, in such a way that it will grow larger and get stronger enough to draw Vortex C across the wake as seen in Figure 1.5(b). This will cause to the shedding of Vortex B. This shedding process will continue by following the same steps each time.

1.1.3 Vortex shedding frequency

If vortex-shedding frequency normalized with the flow velocity U and the cylinder diameter can be easily seen to be a function of Reynolds number on dimensional basis.

$$\boldsymbol{St = St(Re)} \tag{1}$$

in which

$$\boldsymbol{St = \frac{f_v D}{U}} \tag{2}$$

And f_v is vortex-shedding frequency. St which is called Strouhal number is the normalized vortex-shedding frequency. Figure 1.6 shows the relation between Re and St.

As seen on Figure 1.6, the Strouhal number sudden increases at $Re = 3 - 3.5 \times 10^5$ around the critical Re number, from 0.2 to a value about 0.45.

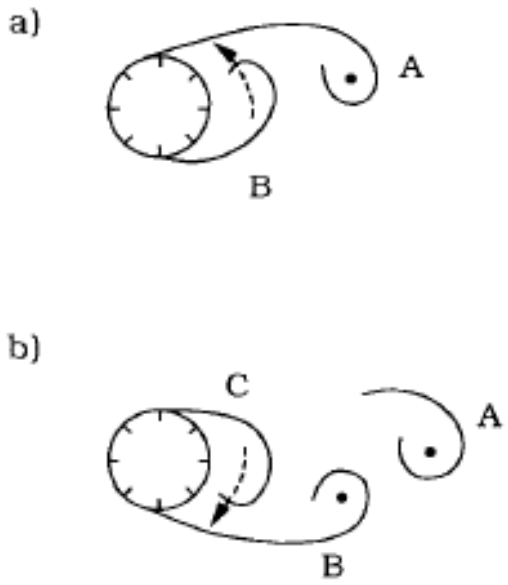

Figure 1.5 : (a): Prior to shedding of Vortex A, Vortex B is being drawn across the wake, (b): Prior to shedding of Vortex B, Vortex C is being drawn across the wake (Sumer & Fredsoe, 2006).

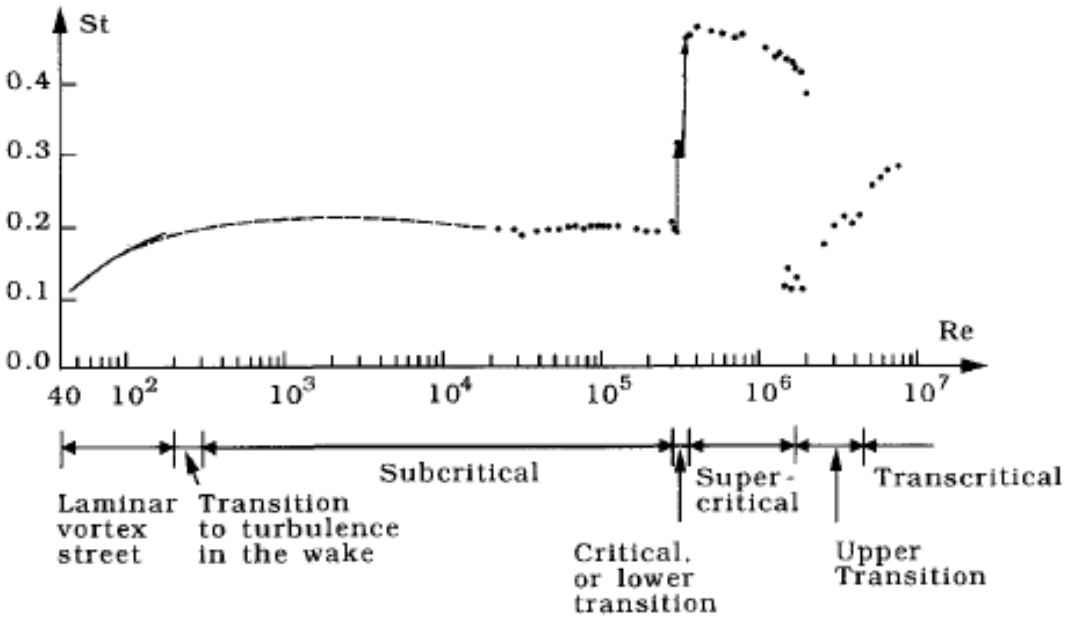

Figure 1.6 : Strouhal number for a smooth circular cylinder. Experimental data from Solid curve: Williamson (1989). Dashed curve: Roshko (1961). Dots: Schewe (1983) (Sumer & Fredsoe, 2006).

1.2 Literature Review

Especially after the industrial revolution, with the effect of urbanization, the way of land use changed dramatically. Consequently, in order to modify the river, societies spent a massive amount of time, money and effort. Factors commonly creating a stress over rivers can be summarized as inappropriate developments in the flood plains, dams which were established for the usage of hydraulic power, river transportation applications, land drainage, flood prevention structures and isolation of water from the bed. According to Brailey and Fryirs (2005) "In the past, quest for security and stability to meet human needs largely overlooked needs of aquatic ecosystems" (p .1). Implementations such as isolating of the rivers from floodplains through floodwalls, channelization programs, cleaning hydrophytes in order to decrease the river roughness can given as examples for this kind of river engineering exercises. Significantly, few river systems preserve their actual condition across the planet (Brierley & Fryirs, 2005). In 2012, European Environment Agency made an announcement explaining, "There are many national examples regarding the major modification of the wetlands, such as Germany. Only 21% of the rivers of Germany preserve its natural state or altered moderately (RESTORE, 2013, p. 5).

Brailey and Fryirs (2006) denotes "In many instances, human activities brought about a suite of unintended and largely unconsidered impacts on river health, compromising the natural variability of rivers, their structural integrity and complexity" (p.1). These changes frequently cause rivers to lose their economic values, create problems regarding flood plain management, waste management and drainage and a lack of quality open space.

As a result of these interventions, community's way of utilizing the rivers and basins changed rapidly, creating an increased attention on the river restoration (Williams, 2001). Especially in the developed countries with the recent increase in environmental awareness, the support for the exploitation of the river resources for economic benefits decreased. Nonetheless, a huge social demand was established regarding the improvement and the management of rivers and wetlands for ecological and environmental benefits. Consequently, this demand caused the comparison and discussion of two important concepts: river engineering and river restoration (Williams, 2001).

Industrial revolution not only brought mechanized industry or technological advantages, but also encourage the idea that human should conquere the nature, utilizate and even exploit of natural resources for the benefit of humankind. A new profession was needed for mankind to achieve its goals which was civil engineering. Moreover, in 1830, in the founding statement of Institute of Civil Engineering it was stated "to harness the great sources of power in the nature for the use and convenience of the man." This passion of the civil engineers to restrain nature was adapted by the river engineers to use the discoveries of science to develop new methods to control or reroute the rivers or utilize the flood plains, irrigate or produce energy (Williams, 2001).

As a result, most of the rivers on earth were, modified by the river engineers in the past century. Increasing evidence shows that actions of river engineers are the main reason behind the environmental deterioration of the rivers and the estuarine ecosystems and they play a significant role in the loss of global biodiversity. The regulation of the flow, isolation of flood plains from river, disconnection of sediment flow and the destruction of riverbank vegetation not only cause an ecological deterioration, but also costs to loss of important economic resources such as commercial fishing (Williams, 2001). It was also observed that the causalities during the natural disasters are increased unexpectedly as result of inconvenient utilization of land caused by the flood prevention (Figure 1.7).

The strong demand regarding the management and rehabilitation of the wetlands and rivers proved the necessity of a new approach in this field and initiated a discussion on the river management. River restoration is an integrated part of the sustainable water management. In this approach, the main aim is to bring objectives such as natural state and the functions of river, land development, recreation and provision of biodiversity together. Restoration means different things to different people. Generally, it refers to the process of supporting the recovery of a damaged or destroyed ecosystem. Balancing the social, economic and environmental needs which are constrained by the existing hydrological, water quality, and sediment tansport regimes of any given system limits these applications (Petts, 1996).According to Williams (2001), one of the supporters of this approach, "Rivers are dynamic evolving physical systems. The river landscape at any given time is an expression of its watershed, climate, geomorphic and ecologic history.

Additionally, rivers have a tendency to recreate an inherent form, and hence are self-correcting. Also the river ecosystem has adapted to this inherent form and the physical processes that sustain it."

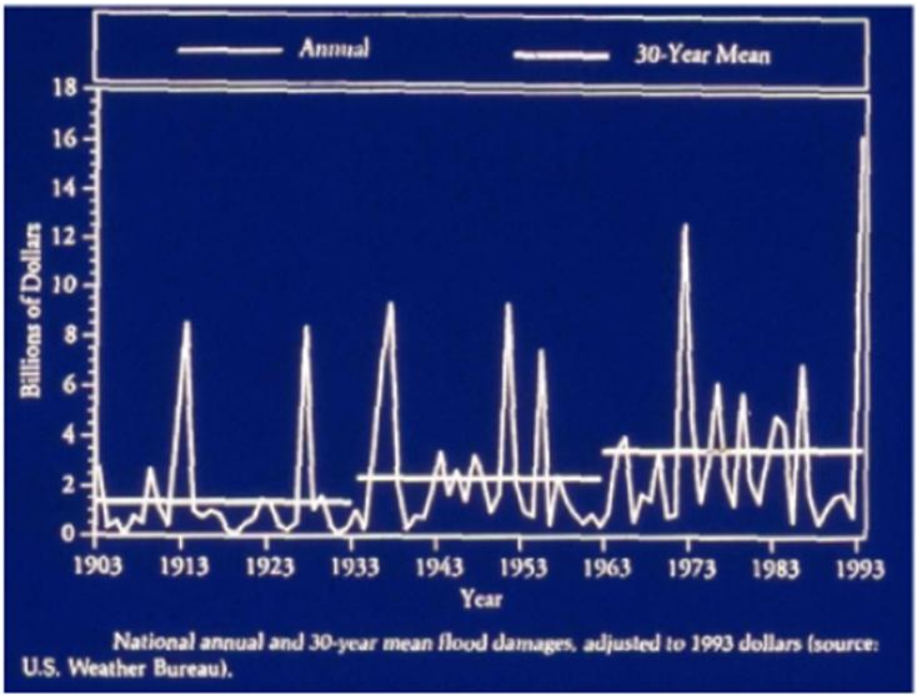

Figure 1.6 : The cumulative effect of the failure of flood control as a substitute for an integrated flood hazard reduction strategy is shown in the escalation of national flood losses (Williams, 2001).

To reverse a river to its natural state creates many benefits such as provision of a healthy developed ecosystem for the society and the environment, establishment of a natural gravitation field. To summarize;

- A quality life, increase in the living standards;

  Creating a connection between the society and the nature by the establishing of new and accessible recreational green spaces; increasing the water quality by obstructing the polluters to blend into the water contribute to the public health.

- Contributes economically;

  Decreases the risk of flood and flood prevention cost. Causes good quality water and low treatment costs.

- Feeds new habitats;

  Reversion of rivers to their natural state and the creation of wetlands enhance new habitats for bird, fishes and other living creatures.

- Combats the climate change and provides a green infrastructure;

  Climate change results in more floods and drought that threatens urban zones, ecosystems and enterprises.

1.2.1 Role of vegetation on aquatic and riparian ecosystems

To understand how to apply an ecological, multi-functional and sustainable river restoration, comprehending deeply the both aquatic and riparian vegetation's role on ecosystems is necessary. Acoording to Gurnell et al. (2012), "Once established, riparian and aquatic plants frequently act as physical ecosystem engineers by trapping and stabilizing sediments, organic matter and the propagules of other plant species, modifying the local sedimentary and morphological environment by driving the development of landforms and associated habitats, and so facilitating the rapid establishment of other plants that can in turn reinforce the development of landforms such as river banks, vegetated islands and floodplains" (p. 1). Aquatic and riparian vegetation have great impacts on river ecosystems as, increasing the bank stability, providing habitat for animals and invertebrates, improving the water quality, building pioneer landforms by trapping and stabilizing sediment, promoting biodiversity and regulating water temperature. Transport and deposition of sediment depending on the frequency and magnitude of river discharge, which also moderated by sediment supply and valley gradient have long been defined as the key control mechanisms on fluvial morphodynamics (Gurnell A. , 2014). Until the second half of the 20th century, these topics were the focus points to understand the river form and dynamics. After 1950s, researchers started to consider vegetation not only an exposed material on rivers but also an active agent on river morphodynamics. That vision was a beginning of an enlightment era on the water-biota-sediment interactions. During the last 60 years, knowledge on this complex process that establishes and enhances a sustainable river ecosystem has builded up over time, due to the increased awareness over the importance of physical influence of living vegetation on fluvial systems. In the first decades of this enlightment era researches frequently performed through field observations, after the late years of twentieth

century theoretical and flume investigations have contributed to the exertion of comprehending the influence of plants on river ecosystems (Gurnell A. , 2014). Gurnell, (2014) denoted that: “In relation to bank erosion/aggradation, important early experiments with silty bank materials by Smith (1976) estimated a 20 000 time increase in erosion resistance when these materials included up to an 18% volume

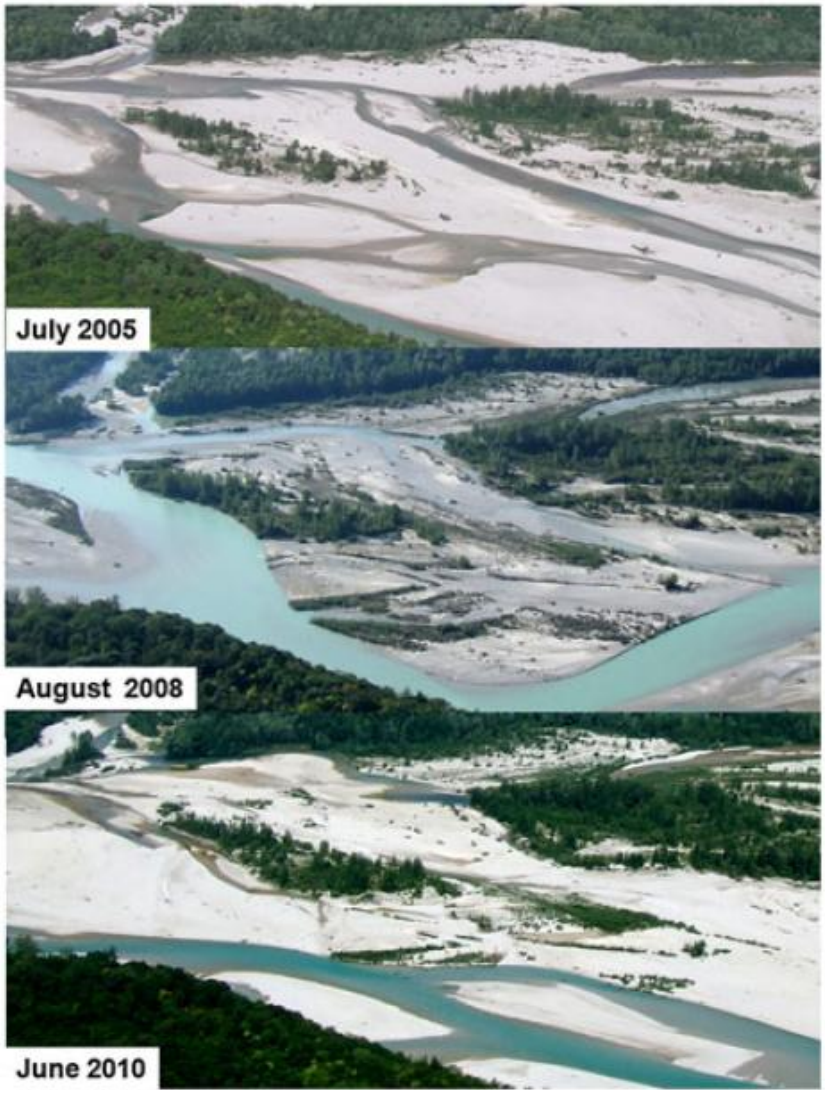

Figure 1.7 : Shifting mosaic of open water, bare gravel, and vegetated patches of different ground cover, biomass, height and species composition at the same site on Tagliamento River in July 2015 (following a bankful flood in winter 2004-2005); in August 2008 (following three years without any significant floods); and June 2010, (following two years with some significant floods, altough none reached bankfull stage) (Gurnell A. , 2014).

root mat”. Simon and Hupp (1990) emphasized the role of vegetation on cross profile recover processes of enlarged and straightened channels by enhancing the sediment

trapping. After major erosive floods on Plum Creek River (Colorado), Friedman et al. (1996) observed channel narrowing because of the sediment retention by colonized vegetations. Due to decrease in riparian vegetation, loss of bank stability and channel widening, even transitions between meandering to braided planforms observed by Kondolf and Curry (1984, 1986) and Madej et al. (1994). Shieds and Gray, (1992) and Dwyer et al. (1997) show riparian vegetation have a significant impact against the erosion of levees. Impacts of vegetation on river channel morphodyamics and planform researched not only through field observations but also via flume experiments. McBride et al. (2007) conducted flume experiments in an attempt to compare the non-forested (synthetic grass carpet) and forested (rigid wooden dowels) riparian vegetation cases. As result of these experiments, Mcbride et al. (2007) observed a narrow band of high turbulence area between main channel and the floodplain for forested riparian condition such that turbulent kinetic energy was twice that of non-forested runs. Which means forested floodplains may result higher channel widths thereby inducing the sediment transport. In overwidened, straight channels nominal patches of emergent vegetation may trigger channel narrowing and increase in meandering (Bennet et al., 2002, 2008; Bennet S. , 2004) according to the flume experiments. In addition, simplification of river planform and persistence of single thread channels are the consequences of vegetation existence by virtue of reinforcing sediment and so diminish channel widening and cutoffs. (Gran & Paola, 2001; Tal et al., 2004; Jang & Shimizu, 2007; Tal & Paola, 2007; Braudrick et al., 2009; Li & Millar, 2011)

As described, vegetation colonization can reinforce the sediment. Beside that because of the flow resistance, which substantially implemented by canopy; sediment, nutrient and plant propagule deposition increases as shown in Figure 1.9. This process leads to vegetative reproduction and spatial extension of vegetation patches in fluvial systems. Svendsen et al. (1998) found that, retention by deposition amounted to 12% of total nutrient export in lowland river system. The highest monthly retention occurred in summer and reached values of 25% of total phosphorus load. Also in another research by Schulz et al. (2003), mean load-weighted phosphorus retention and nitrogen retention were 12.2% and 2.5% respectively. According to Schulz et al. (2003, p.577), “Deposition is the major process, which causes phosphorus retention in the lower River Spree”. In this

research Schulz et al. (2003) obtain that “Low flow velocities coincide with extend deposits of particulate organic matter within and downstream of macrophyte stocks. Macrophytes significantly reduced flow velocities, and therefore improved conditions for the settlement of organic seston”.

Gurnell (2012), denotes that “However, there appear to be a few plant species that are particularly well equipped to initiate vegetated patches within disturbed riparian corridors across a wide range of river environments. These physical ecosystem engineers can influence vegetation dynamics by creating and modifying habitats and facilitating colonization by other plant species in river systems with sufficient suspended sediment supply for habitat or landform building. They have a crucial impact on sediment stabilization and pioneer landform building at the interface between the plant (resistance) dominated and fluvial-disturbance (force) dominated zones of the river corridor (Figure 1.10)” (p.134).

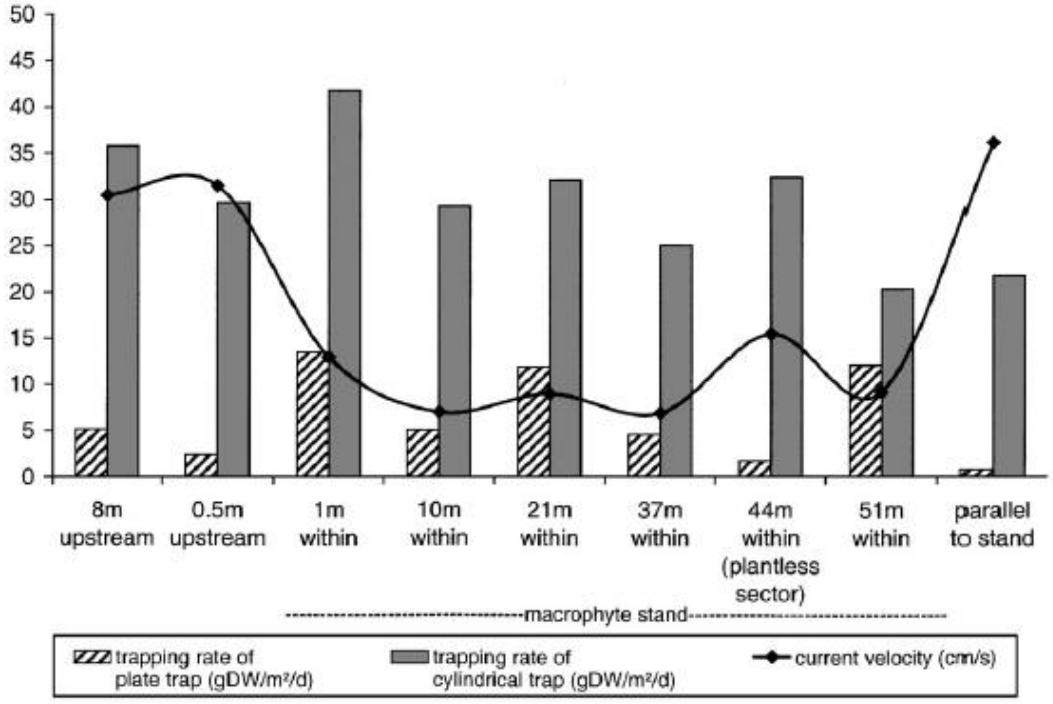

Figure 1.8 : Longitudinal section upstream of and within a macrophyte stand, showing trapping rates measured with cylindrical and plate traps and flow velocity (Gurnell A. , 2014).

The most various, dynamic, and complicated habitats on the land portion of the earth are natural riparian corridors. Riparian corridors are the interfaces of terrestrial and aquatic ecosystems where richest ecological processes, sudden changes take place.

Within the larger landscape riparian corridors affects the diversity of landforms, communities and environment (Naimann et al., 1988, Gregory et al., 1991).

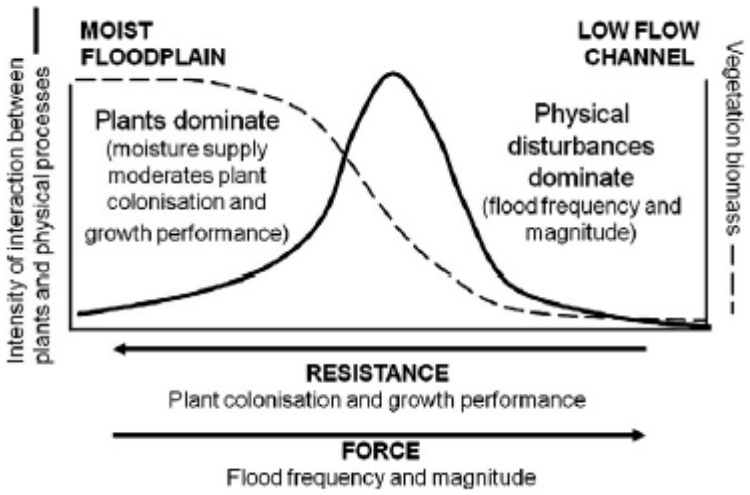

Figure 1.9 : Zone of intense interaction between plants and physical processes at the junction between plant dominated and flood disturbance dominated zones of a humid temperature river corridor. The position of the zone of interaction shifts with adjustments in plant growth performance and flood disturbance and the character of the interaction zone is heavily affected by pioneer landform construction(Gurnell A. , 2014).

According to ecological investigations on riparian corridors, their significant regulator roles on environmental vitality are clearer. Riparian vegetation affects temperature and light regimes, supply nutrients to aquatic and terrestrial biota, maintains biodiversity, and regulates the flow and nutrients that are travelled through the river from the uplands (Naiman & Decamps, 1990). About three-quarter of vertebrate species in a region use riparian corridors in their life cycles in some significant way (Raedeke, 1989). For instance, Nilsson (1992) reports %13 (>260 species) of the entire Swedish flora of vascular plants are located along a single river corridor; Junk (1989) reports that all periodically flooded forests in Amazon basin may have ≈20% of the 4,000-5,000 estimated Amazonian tree species; and Tabacchi et al. (1990) report over 900 taxa of vascular plants along the Adour River riparian corridor in France.

Another role of riparian or aquatic vegetation is denitrification. Nitrogen levels on aquatic systems increased dramatically in the past decades. Excess nutrient concentration leads various problems such as phytoplankton blooms, hypoxia, and loss of biodiversity in aquatic ecosystems worldwide. Denitrification means the

removal of nitrate from aquatic system by reduction to gaseos nitrogen. Several researches that are about direct comparison between vegetated and non-vegetated conditions showed positive effects of macrophytes on denitrification (Christensen and Sorensen 1986; Nielsen et al. 1990; Sündback and Miles 2002).

1.2.2 Flow through porous obstruction

The knowledge acquired by the studies (Graf & Yulistiyano, 1998; Roulund et al., 2005; Unger & Hager, 2007) investigating the flow around cylindrical piles may be evaluated to understand the process for relatively large individual vegetation elements. The flow decelerates and a strong downflow appears when flow approaching to cylindirical piles. This deceleration and downflow behavior cause the formation of horseshoe vortex at the base. As it mentioned in Chapter 1.2.3, streamlines are contracted, shear layer around the obstacle is formed and the turbulence generation is increased while flow passes around the obstacle. Following, this turbulent condition feed the shear layer formed downstream of the separation point and causes to vortices called lee-wake vortices. Lee-wake vortices propagates downstream with the occurrence of the vortex shedding and carve out the vortex street. Bleed-flow, which delays the beginning of the von Karman vortex street, is the main difference between the flow over porous and solid obstacles. Zong and Nepf (2012) observed a region of uniform velocity, which is called "steady wake region" downstream of the obstacle. Just afer the obstacle streamwise velocity decreases slightly, beyond a point $\bar{u}$ is constant until the end of the steady wake region. This behavior shows that, in that specific region there is not any form of mixing between the bleed-flow and the contracted flow until the two shear layers, which are triggered on the both sides of the obstacle, intersect.

Several studies such as Nicolle and Eames (2011), Chen et al. (2012), Zong and Nepf (2012) investigated the flow behavior over such a porous array. Researches like Takemura and Tanaka (2007), Tanaka and Yagisawa (2010) used several configurations of similar porous obstacles and recognized their influences depending on the porosity. The array density identified as L/d, where L is the space between neighboring cylinders and d is the cylinder diameter. In terms of producing a large-scale von Karman vortex street; if $L/d < 1$ which specify too low porosity, the structure behaves more similarly to an equivalent diameter rigid cylinder. Otherwise

if the porosity is too high $(L/d > 5)$, as like as individual piles primitive von Karman streets are occurred behind each individual cylinder.

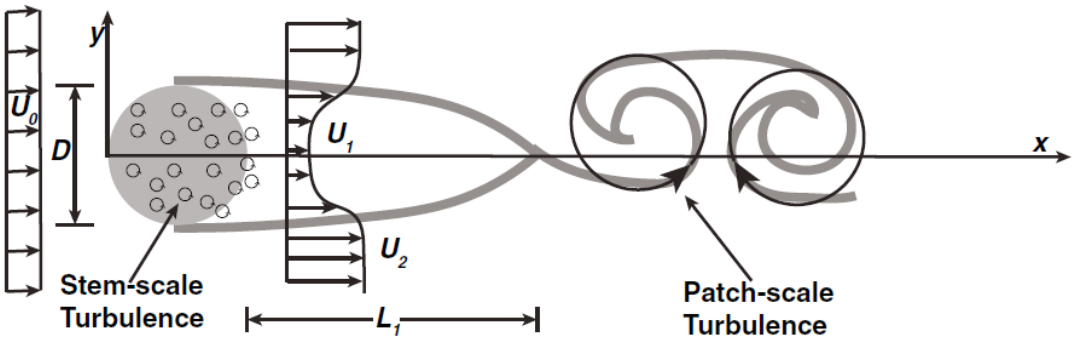

Figure 1.10 : Upstream velocity, U_0 , adjusts to patch of emergent vegetation, diameter D, producing a wake profile with velocities ($U_1$and U_2) shown in streamwise, x and lateral, y, directions. The grey lines represent dye streaks (shear layers). The steady wake zone is denoted by length L_1 (Zong & Nepf, 2012).

1.2.3 Relationship between drag force and turbulence

The easiest and funniest way to explain the relation of drag force with the changing turbuluence is referring to golf ball aerodynamics. We have mentioned the flow seperation in Chapter 1.1.2, additional information is that, the drag on a body is dominated by the flow seperation over its surface. If the seperation minimized the experienced drag would be significantly reduced. Golf ball is a great example to understand this behavior.

Figure 1.12 shows how the drag changes with Re for dimpled and smooth spheres which have the same geometry. Since the laminar boundary layer around the smooth sphere separates so rapidly, it creates a very large wake over the entire rear face. This large wake maximizes the region of low pressure and, therefore, results in the maximum difference in pressure between the front and rear faces. As we have seen, this difference creates a large drag like that seen below the transition Reynolds number. The transition to a turbulent boundary layer, on the other hand, adds energy to the flow allowing it to remain attached to the surface of the sphere further aft. Since separation is delayed, the resulting wake is much narrower. This thin wake reduces the low-pressure region on the rear face and reduces the difference in pressure between the front and back of the sphere. This smaller difference in pressure

creates a smaller drag force comparable to that seen above the transition Reynolds number. Afforementioned behavior can be seen in Figure 1.13.

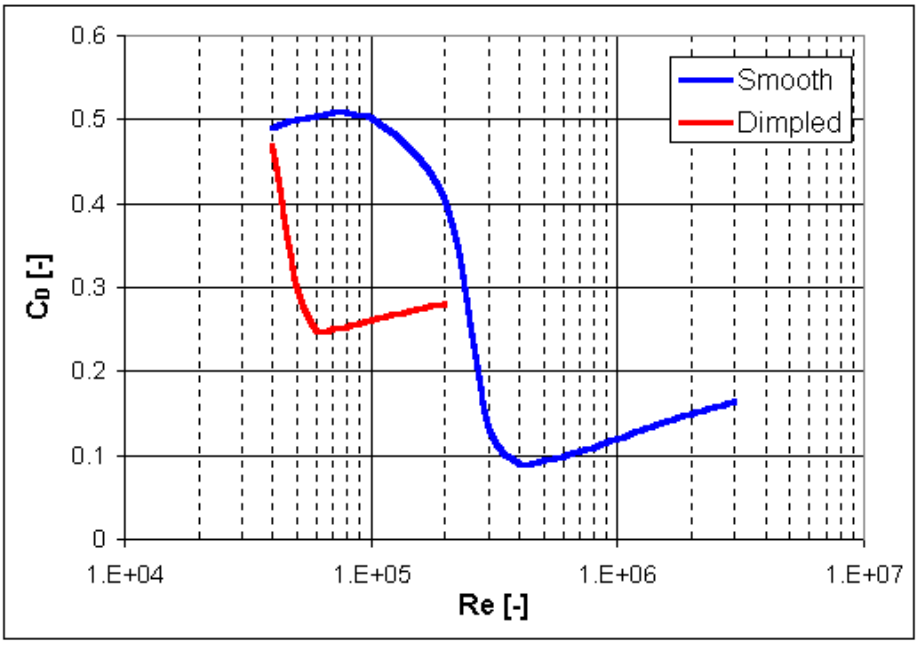

Figure 1.12 : Variation of drag coefficient with Reynolds number for dimpled and smooth spheres. (Aerospaceweb, 2015)

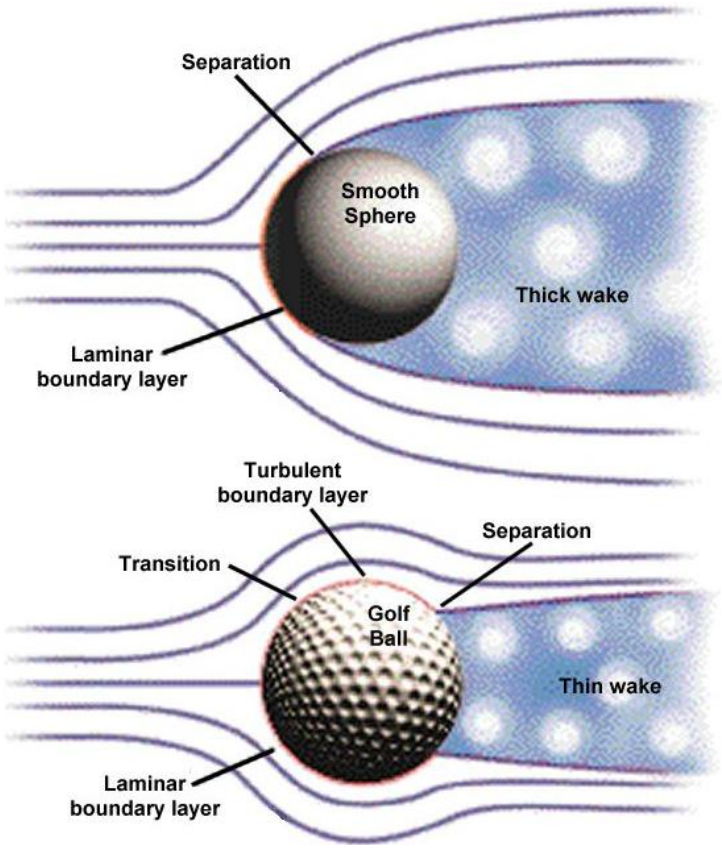

Figure 1.11: Flow seperation on a sphere with a laminar versus turbulent boundary layer. (Aerospaceweb, 2015)

With the help of the golf ball example, now we can mention the circular cylinder geometries in flow field. The same approach is valid for circular cylinders also, as it can be seen in Figure 1.14. Also the pressure distribution change with the changing Re can be seen in Figure 1.15.

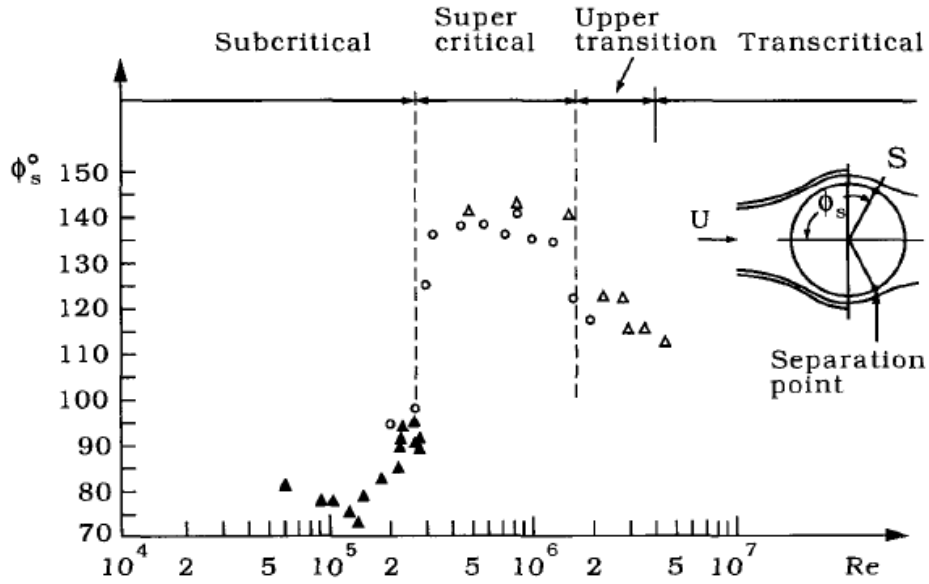

Figure 1.13 : Position of the separation point as a function of the Reynolds number for circular cylinder. Achenbach (1968)

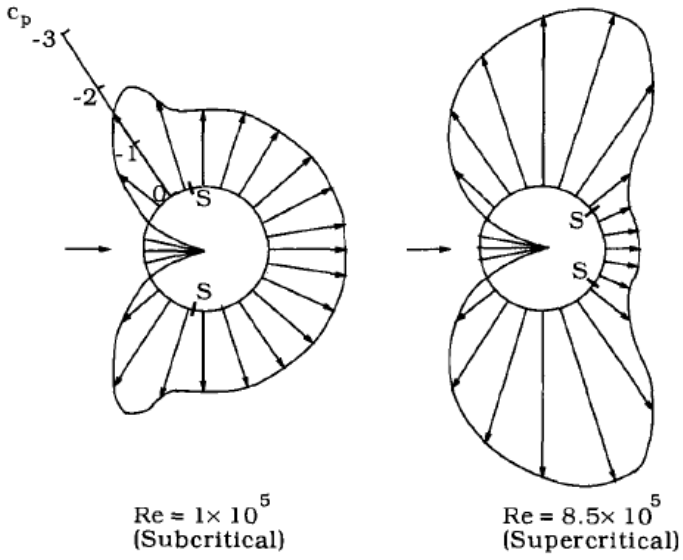

Figure 1.14: Pressure disributions around circular cylinders in different Reynolds number conditions. S denotes the seperation point. Achenbach (1968).

2. EXPERIMENTAL SETUP

2.1 Experimental Facilities

The flume experiments were conducted in the Istanbul Technical University Hydraulic Laboratory. The flume is 26 m long, 0.98 m wide, and 0.85 m deep as can be seen on Figure 2.1. The bed is smooth concrete (horizontal) and sidewalls are Plexiglas. By a flow straightener system with honeycomb pattern that covering the whole flume width and depth at upstream end of flume smooth inlet conditions were provided. A tailgate weir at downstream end of the flume used to control the water depth. Separate internal and external flow circulation systems used to adjust the flow conditions that needed. The external pump has a capacity of 25 kW and is used for elevating the water to a reservoir 17m above the flume. The desired flow transmitted by the effect of gravitation and it can be easily set by a ball valve. A pump with 5kW capacity provides the internal recirculation. Both pumps were utilized simultaneously to carry out this experiment. The flow discharge was set to $Q = 100 l/s$ and the flow depth $h = 31.1\, cm$, resulting a cross-sectional average flow velocity of $U_\infty = 0.33\, m/s$. The Reynolds number for uniform cylinder was $5{,}3 \times 10^4$.

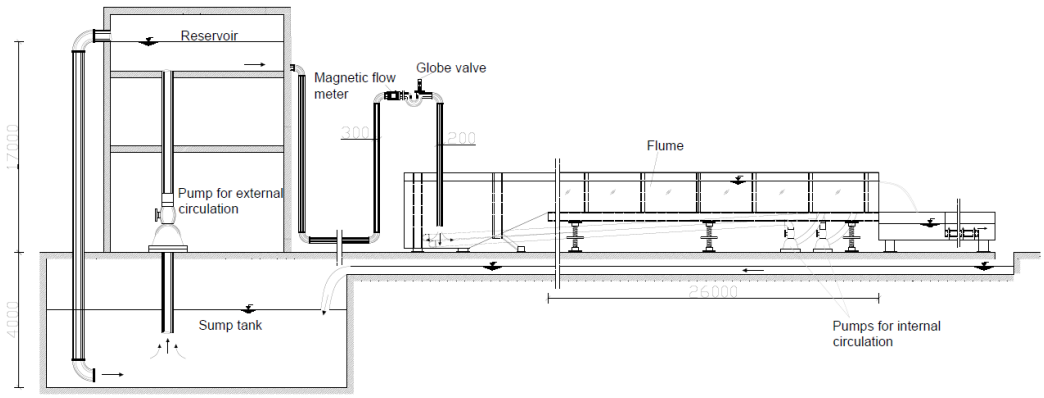

Figure 2.1 : The utilized flume and its recirculation system.

2.2 Artificial Vegetation Charactheristics

The obstacles were placed at the centerline of the flume, approximately 11 mdownstream from the flume inlet, where fully developed turbulent flow conditions attained. Flow depth is set to $h = 31.1$ cm and it is observed in both downstream and upstream of the obstacle during the experiments. The vegetation like elements became gradually more complicated in order to compare the turbulence statistics and to identify the similarities and differences. Firstly, 16 cm diameter rigid emergent circular cylinder is studied to benefit from the available knowledge for this well-known case and quantitively compare the flow pattern with more complicated cases. Then by, as a representation of permeable form of the rigid circular cylinder, hexagonal array of emergent circular cylinders in staggered array are used as shown in Figure 2.2. Afterwards to study the canopy effect, the rigid circular cylinder and the two arrays of circular cylinders used as canopies. A 1.7 cm diameter and 7.5 cm height wooden rod supports them. In this case, the ratio of trunk to canopy is 1:4, within the flow depth. As a result, complicated flow patterns generated by porous obstacles investigated with the first tree configuration, while with the latter configuration also the subcanpoy affect took in consideration.

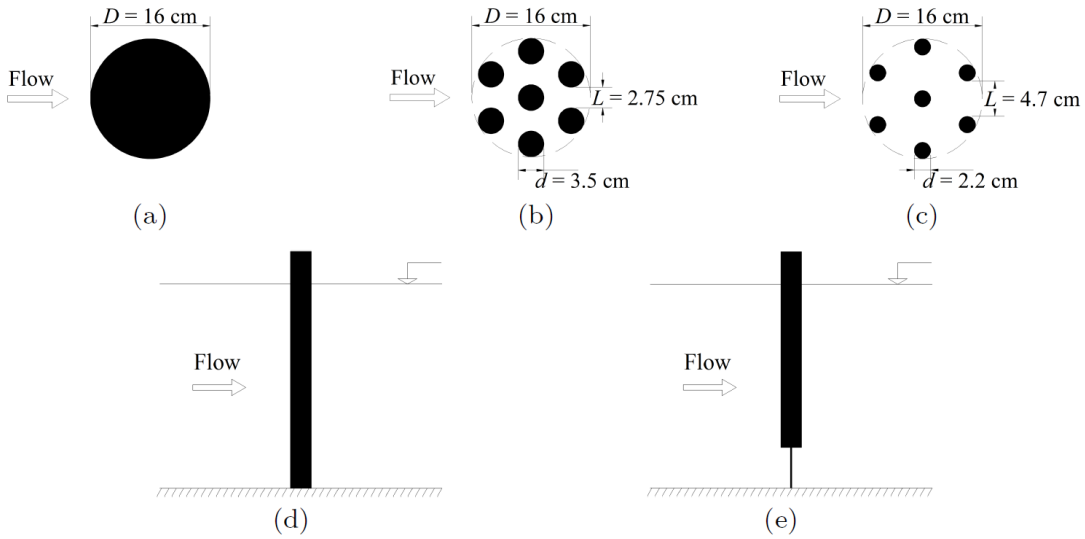

Figure 2.2 : The (a) rigid cylinder (b) dense and (c) sparse hexagonal array of circular cylinders in staggered arrangement, which served as (d) a uniform emergent obstacle or as (e) the vegetation canopy. The dashed circumference in (b) and (c) shows the fictional perimeter.

To be able to compare the real vegetation behavior with artificial vegetations, a vegetation (*Cupressus macrocarpa)* used which has the same trunk to ratio canopy which is shown in Figure 2.3. Also some fotographs of experimental facilities and obstacles are shown in Figures 2.4, 2.5, 2.6 and 2.7.

Figure 2.3 : Vegetation (*Cupressus macrocarpa*) which is used in experiments to compare the behavior with artificial vegetations.

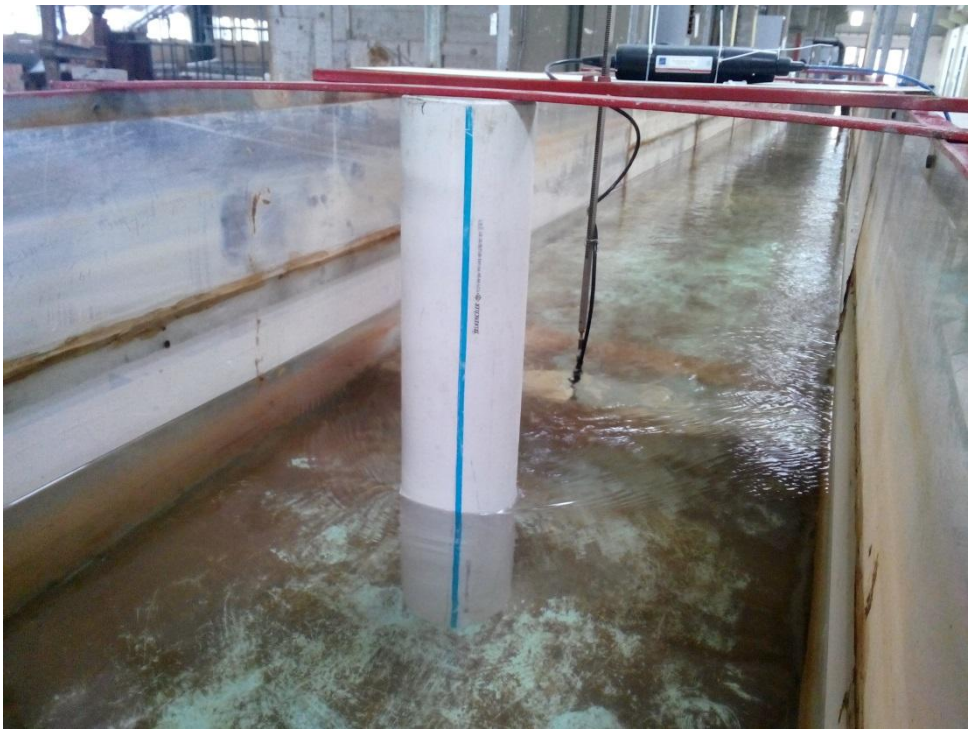

Figure 2.4 : Experimental facilities of uniform cylinder experiments.

Figure 2.5 : Experimental facilities of uniform dense array experiments

Figure 2.6 : Appearance of the tree-like cylinder in flume. (*Cupressus macrocarpa*).

Figure 2.7 : Appearance of the tree-like cylinder in flume.

2.3 Flow Velocity Measurements

The velocity measurements conducted by a Vectrino II Acoustic Doppler Velocimeter (ADV), manufactured by Nortek. The ADV mounted on a moveable platform over the flume, which is able to move in longitudinal and transverse direction. The vertical adjustment of the device was set according to a custom-made positioning system. The sampling duration was 100 s, sampling frequency set to 100 Hz and the height of the sampling volume was set in the range of 1.2 cm to 1.9 cm according to position of transducer and flow velocity. Such velocity measurements inevitably include noise resulting into spikes in the retrieved time-series data. These spikes were considered outliers and were removed according to the methodology suggested by Goring and Nikora (2002) and the MATLAB code provided by Wahl (2003) and Mori et al. (2007). The velocity measurements were conducted for the grid shown in Figure 2.4. Measurements were taken at thirteen spots along the longitudinal direction and nine depthwise. In addition, velocity measurements were conducted at the center of the right side, at six points depthwise at selected longitudinal spots to examine the momentum transfer in transverse direction.

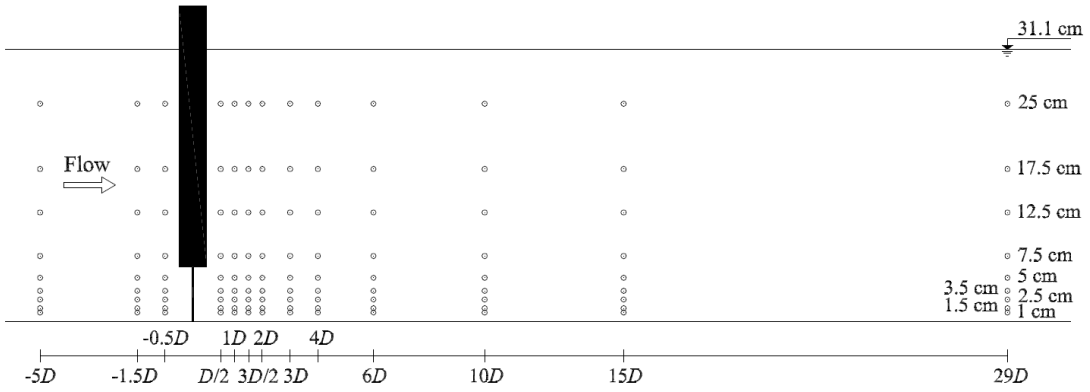

Figure 2.8 : Grid of the flow velocity measurements along the flume centerline. The noted longitudinal distance measured from obstacle edge while the vertical distances exaggerated for illustration purposes.

2.4 The Influence of Sampling Number on Turbulence Statistics

Before starting the experiments, determining the required sampling number was essential. Some preliminary tests conducted with the dense array for obtaining the necessary sampling number to represent the real conditions. In these preliminary experiments, 5 minutes long data, which is believed long enough, collected in 100

Hz just 2 cm behind the obstacle and 1 cm above to the bed where the turbulence predicted to be maximum. For each sampling number, time averaged velocities ($\overline{u}$, $\overline{v}$, $\overline{w}$), fluctuating velocity components (u', v', w') and turbulence kinetic energy and their confidence interval levels for confidence level 0.95 calculated and presented in fig. As seen on figures, the confidence interval relatively wider for the sampling number lower than 5000 in comparison with higher sampling numbers. In the light of this information, each measurement duration had chosen 100 seconds, which represent 10000 sampling number, to stay in the safe zone. After whole experiments conducted, most turbulent location obtained at uniform cylinder configuration. ($x/D = 1{,}5$ and $z = 17{,}5\ cm$). 10 minutes long data collected at that point and same analysis applied on those data to understand if the selected sampling number represent the real conditions.

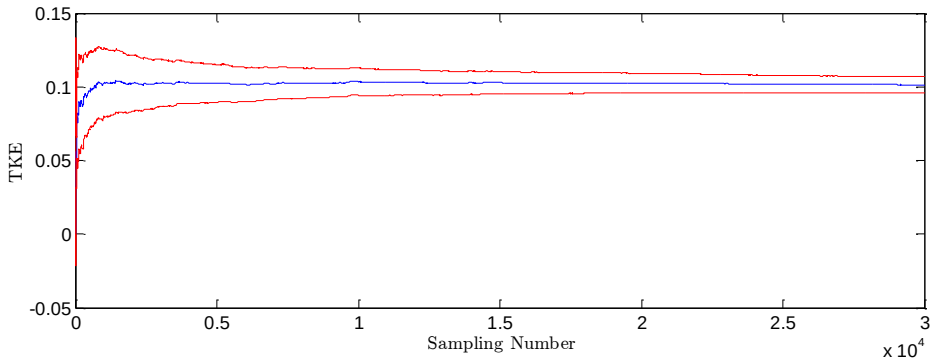

Figure 2.9 : Mean turbulence kinetic energy by changing sampling number at $x/D = 1{,}5$ and $z = 17{,}5\ cm$ for uniform cylinder which was the most turbulent point of whole experiments.

3. ANALYSIS OF RESULTS AND DISCUSSION

The instantaneous velocity measurements, which are taken by ADV, are noted as u for the streamwise, v for the transverse and w for the vertical direction flow velocity. These instantaneous flow velocities contain both time averaged velocities ($\overline{u}, \overline{v}, \overline{w}$) and fluctuating velocity components (u', v', w'), according to Reynolds decomposition $u = \bar{u} + u'$, and likewise for v and w. The equation of flow turbulence kinetic energy per unit mass (TKE) is defined as:

$$\boldsymbol{TKE = \frac{1}{2}(u_{rms}^2 + v_{rms}^2 + w_{rms}^2)} \tag{3}$$

where $u_{rms} = \sqrt{\overline{u'^2}}$ is the streamwise turbulence intensity, and similarly, v_{rms} and w_{rms} are the transverse and vertical turbulence intensities, respectively. In order to make the variables dimensionless, all velocity and energy data based variables normalized with the depth and time averaged streamwise velocity U_∞ at the furthermost upstream, where the flow considered to be undisturbed. The longitudinal distances are denominated in obstacle diameter D. Besides the vertical measurement points normalized with constant flow depth h.

In the present study, the two considered arrays have $L/d = 2.75/3.5 = 0.77$ for the sparse array and $L/d = 4.7/2.2 = 2.13$ for dense array, as can be seen in Figure 2.2.In Takemura & Tanaka (2007), the $L/d = 0.5$ and $L/d = 3.0$ for the sparser and denser array, respectively. Similar to Zong and Nepf (2012), the density of cylinders can also described by the solid volume fraction $\emptyset$ which is equal to $\emptyset = n\pi d^2/\pi D^2$, where n is the number of cylinders and D is the embracing cylinder diameter. In present study the solid volume fraction for the dense array is $\emptyset = 0.335$ and for the sparse array is $\emptyset = 0.132$.

In this section the findings of the present study is presented. Figure 3.2 and 3.3 show the mean streamwise velocity profiles for all the studied cases. In each subfigure the velocity profiles obtained for flow over the depthwise uniform emergent obstacle are

depicted together with those generated from tree-like vegetation where the same obstacle served as the canopy. For all the cases, at $-5D$ the logarithmic velocity profile is considered to be similar to the undisturbed flow profile.

At the immediate vicinity of downstream of the obstacles, the streamwise flow velocity decreases dramatically because of the drag induced separation phenomenon, which is mentioned in Chapter 1.2.2. With the increasing porosity, existence of the bleed-flow reduces the deceleration effect. Even in uniform cylinder condition, the decelaration is not distributed homogenously on the vertical direction. As it shown in Figure 3.2(a) the flow velocities near the surface are negative but velocities near the bed are so close to zero or even have positive values. This difference may be explained with horseshoe vortex phenomena .With the increasing turbulence near the bed based upon horseshoe vortex, the separation delays and the adverse pressure gradient zone shrinks at the downstream end of the obstacle. In case where the flow is turbulent, the increased transfer of momentum due to the Reynolds stresses from the free-stream to the wall increases the streamwise momentum in the boundary layer. This allows the flow to suppress the adverse pressure gradient at the downstream surface of obstacle relatively (Figure (1.14) and 1.15). It does not inhibit the separation but delays it further downstream as can be seen in Figure 1.14. Negative flow velocities may not exist as a result of the limited adverse pressure gradient due to the higher turbulence at base of the obstacle where horseshoe vortices occurred. In addition, the behavior near the surface may be explained with the insufficiency of turbulence which couldnot suppress the separation and adverse pressure gradient.

When cross-profile mean velocity taken account, the Reynolds Number near the uniform cylinder is about $Re = 5.2 \times 10^4$. With respect to Figure 1.14 flow near the cylinder corresponds to subcritical region, but with the horseshoe vortex effect it may fit in super critical or upper transition zones near the bed. In the light of this information, a dissertation came up as “in depthwise direction, separation point delays for cylindirical piles” (Figure 3.1).

Below $z/h = 0.2$ where represents the bottom side of canopy, flow starts to accelerate from $0.5D$ upstream of the obstacle for the tree like vegetation model when compared to the uniform obstacles. This acceleration attributed to the

subcanopy flow. By virtue of the higher blockage area of solid cylinder, flow acceleration is more significant than the porous tree-like obstacles.

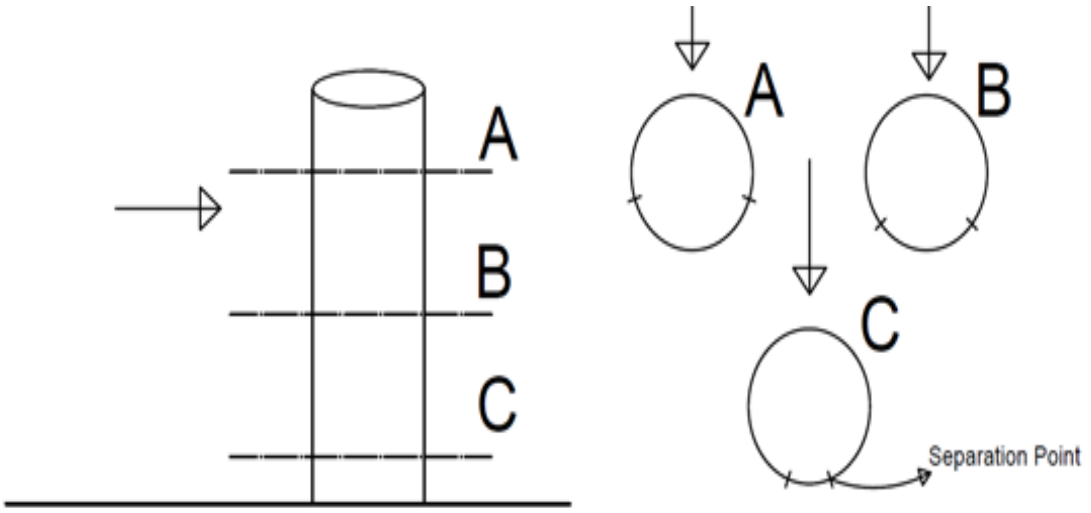

Figure 3.1: Probable variation of seperation point in depthwise direction. Lines behind the cylinders denote separation points.

It is obvious on Figure 3.2(a) the strongest subcanopy jet flow occurred when the solid cylinder is served as the canopy. With the increasing porosity of the canopy, downflow and subcanopy flow intensity decreases with the existence of bleed-flow as shown in Figures 3.2 (b) and Figure 3.3.

Moreover, the existence of subcanopy flow leads higher flow differences between the downstream of canopy and the trunk as indicated in Yagci et al. (2010). Because of this steep velocity gradient, shear induced vertical turbulent mixing increases in all cases, which leads to quicker flow recovery compared with to the uniform obstacles in immediate vicinity downstream of obstacle. As seen on Figure 3.1(a) just behind the obstacle $(0.5D)$ flow velocities over $z/h = 0.4$ are around same values but till $4D$ there are significant differences between those velocity values. This behavior shows that the role of the vertical turbulent mixing (momentum transfer) according to velocity gradient. In this case lateral momentum transfer also assumed to be as a reason of the mixing but over $z/h = 0.4$ velocity gradient in lateral direction are similar between uniform cylinder and tree-like cylinder at $x = 0.5D$ as can be seen in Figure 3.4.

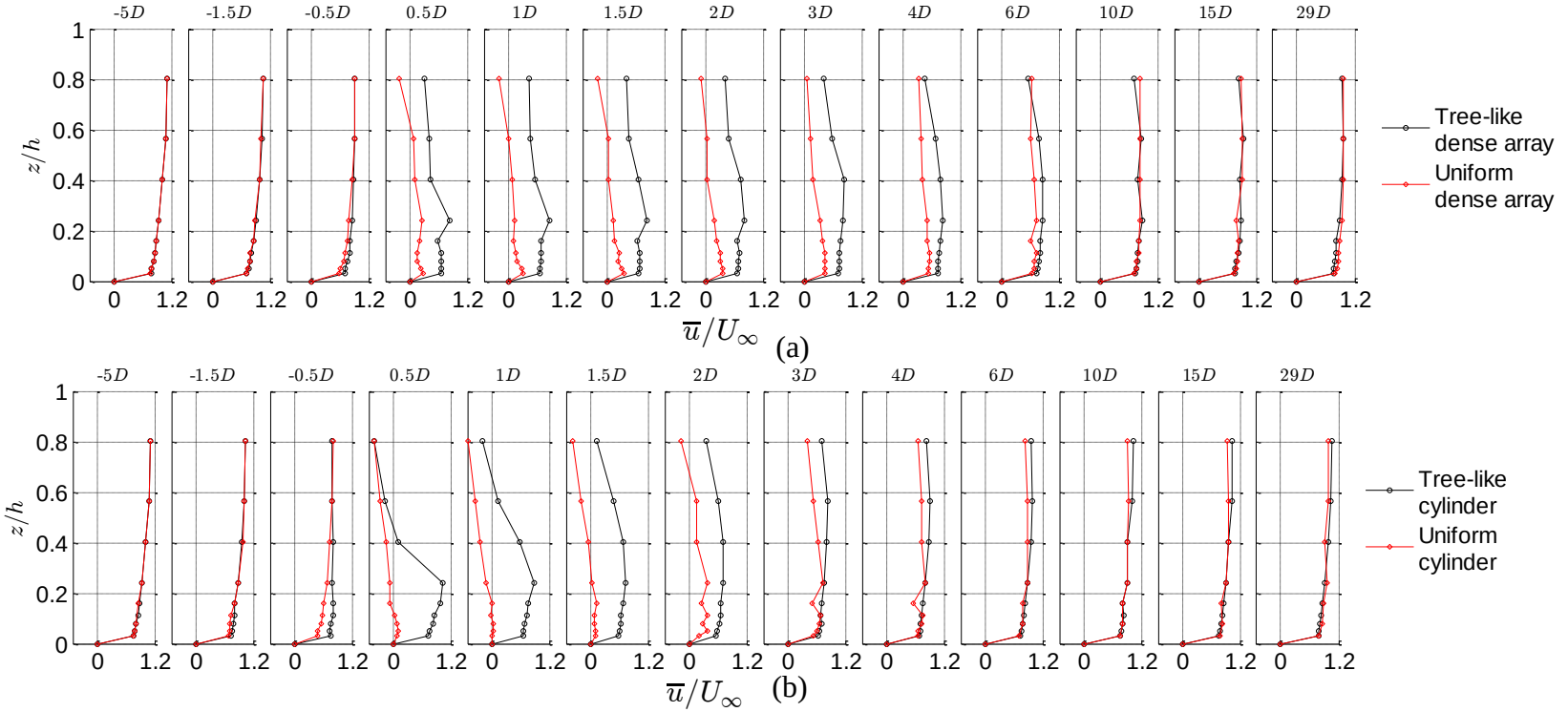

Figure 3.2 : Mean normalized streamwise flow velocity $\bar{u}$ profiles for flow over depthwise uniformly shaped emergent obstacle and the corresponding tree-like vegetation where the same obstacele served as the canopy. The obstacle was (a) a rigid cylinder, (b) the dense array of Figure 2.2. The heading of each subfigure denotes the distance from obstacle edge, while the bottom side of the canopy is at $z/h = 0.2$.

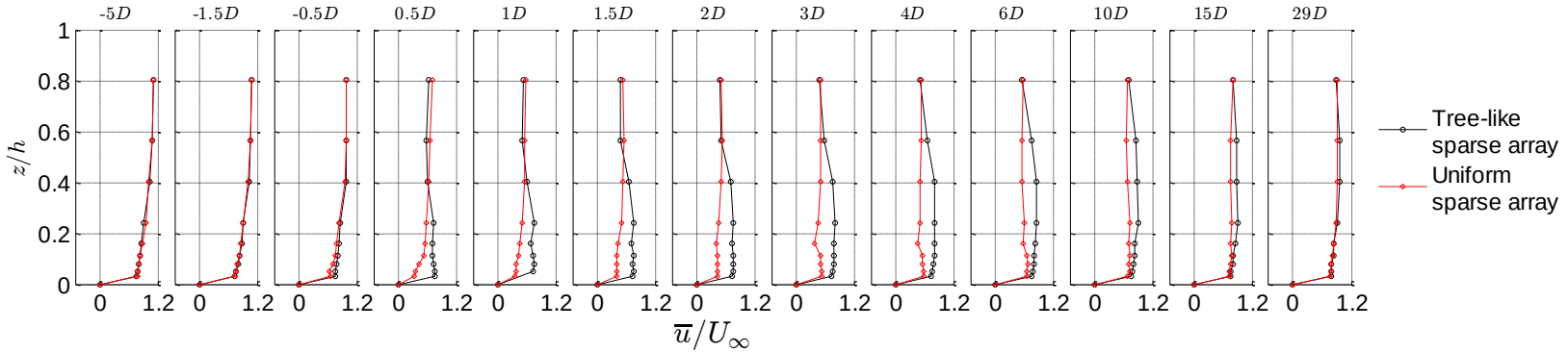

Figure 3.3 : Mean normalized streamwise flow velocity $\bar{u}$ profiles for flow over depthwise uniformly shaped emergent obstacle and the corresponding tree-like vegetation where the same obstacele served as the canopy. The obstacle was the sparse array of Figure 2.2. The heading of each subfigure denotes the distance from obstacle edge, while the bottom side of the canopy is at $z/h = 0.2$.

Another evidence for this assertion is that, downstream of $x = 1.5D$ where velocity gradient in vertical direction for tree-like cylinder is near to disappears, recovery speed for uniform cylinder gets higher than the tree-like cylinder with the effect of velocity gradient in lateral direction.

Zong and Nepf (2012), demonstrated that the bleed-flow spreading from emergent porous structures delays the inception of the patch scale von Karman vortex street, and in it's presence, the flow needs longer distance to recover compared to a rigid emergent cylinder of the same diameter. The results of the present study agree with these findings, as well as to those Valyrakis et al. (2015), as can be inferred from Figures 3.1 and 3.2 when comparing the uniform vegetal elements velocity profiles.

Figure 3.4 and 3.5 shows the lateral turbulence intensity v_{rms} profiles, Figure 3.6 and 4.7 shows mean normalized vertical flow velocity $\bar{w}$ profiles for all the studied cases. In each subfigure the velocity profiles obtained for flow over the depthwise uniform emergent obstacle are depicted together with those generated from tree-like vegetation where the same obstacle served as the canopy. For all the cases, at $-5D$ the logarithmic velocity profile is considered similar to the undisturbed flow profile.

In Figure 3.4, a substantial difference cannot be seen at the immidiate vicinity downstream of the obstacles until around $x/D = 1$ even for trunk region. However, in both cases of solid cylinder and dense array the lateral turbulence intensities of uniform cases are much higher than the tree-like cases in far downstream. Intensity values belonging to the dense array are less than the uniform cases unsurprisingly, but the progression forms are nearly same for both. For the sparse array cases, there is no significant difference between uniform and tree-like obstacles. Nevertheless, subcanopy flow seems to diminish the lateral turbulence intensities at the rear side of the vegetation except sparse array in Figure 3.4. Because of the subcanopy flow, streamwise flow velocity recovers in a shorter distance. As a result of this, the streamwise flow velocity differences in lateral direction at the rear side of obstacle diminishes earlier. Subsequently, lateral turbulence intensities belonging to the case of uniform vegetations are higher than the case of tree-like vegetations at the far downstream. In both comparisons, recovery of lateral turbulence intensity requires longer distance for uniform conditions. If an assumption is made as, the lateral turbulence intensity related with von Karman vortex street, then according to late recover in uniform vegetation von Karman vortex street could extends longer.

However, flow visualization as well as further data is necessary to prove this assertation.

Figure 3.6 and 4.7 shows that in uniform and tree-like vegetations, for all the arrays significant downflow occurs just at the upstream of the obstacles. However, for tree-like vegetations this effect is much more pronounced. The downflow strength diminishes by increasing porosity because of the decreasing area and the existence of bleed-flow. At $x/D = 0.5$ the existence of vertical flow towards water surface is obvious. For uniform obstacles, this upflow starts near the bed because of the horseshoe vortex effect. But in tree-like vegetations the strongest upflow seen in the interface between the trunk and canopy region around $z/h = 0.2$. After $x/D = 1$ uprighted transverse flow for both tree-like solid cylinder and sparse array higher than the uniforms. However in dense array, until $x/D = 2$ the uniform cylinder occurs stronger upflow than tree-like vegetation. For all cases, transverse velocity recovers later than for tree-like vegetation. Also the increasing porosity delays the fully recover of transvere velocity. In the sparse tree-like condition which is the most porose one, transverse velocity doesn't recover until $x/D = 15$.

The time averaged streamwise velocity and turbulence intensity profiles belonging to the three tree-like vegetation and real vegetation cases can be seen in Figures 3.8, 4.9 and 4.10 respectively. The $\bar{u}$ and $\overline{w}$ profiles for the cylinder canopy recover in a shorter distance similar to the finding for uniform obstacles, despite the fact that the cylinder canopy is the only one inducing negative flow velocity close to the surface.Both in real vegetation and porous tree-like relatives, because of the bleed flow, adverse flow velocities inhibited. Aforementioned process is also valid when comparing the tree-like obstacles. The velocity deficit immediate behind the obstacle generates a shear layer that triggers rapid and strong vertical and lateral mixing, which in this case is significantly enhanced by the strong subcanopy flow. Figure 3.8(a) shows that, when the porosity increased for tree-like objects, the time flow recovery takes much longer distance. The reason behind it is smooth gradients between flow layers both lateral and vertical, which are created by the obstruction body.

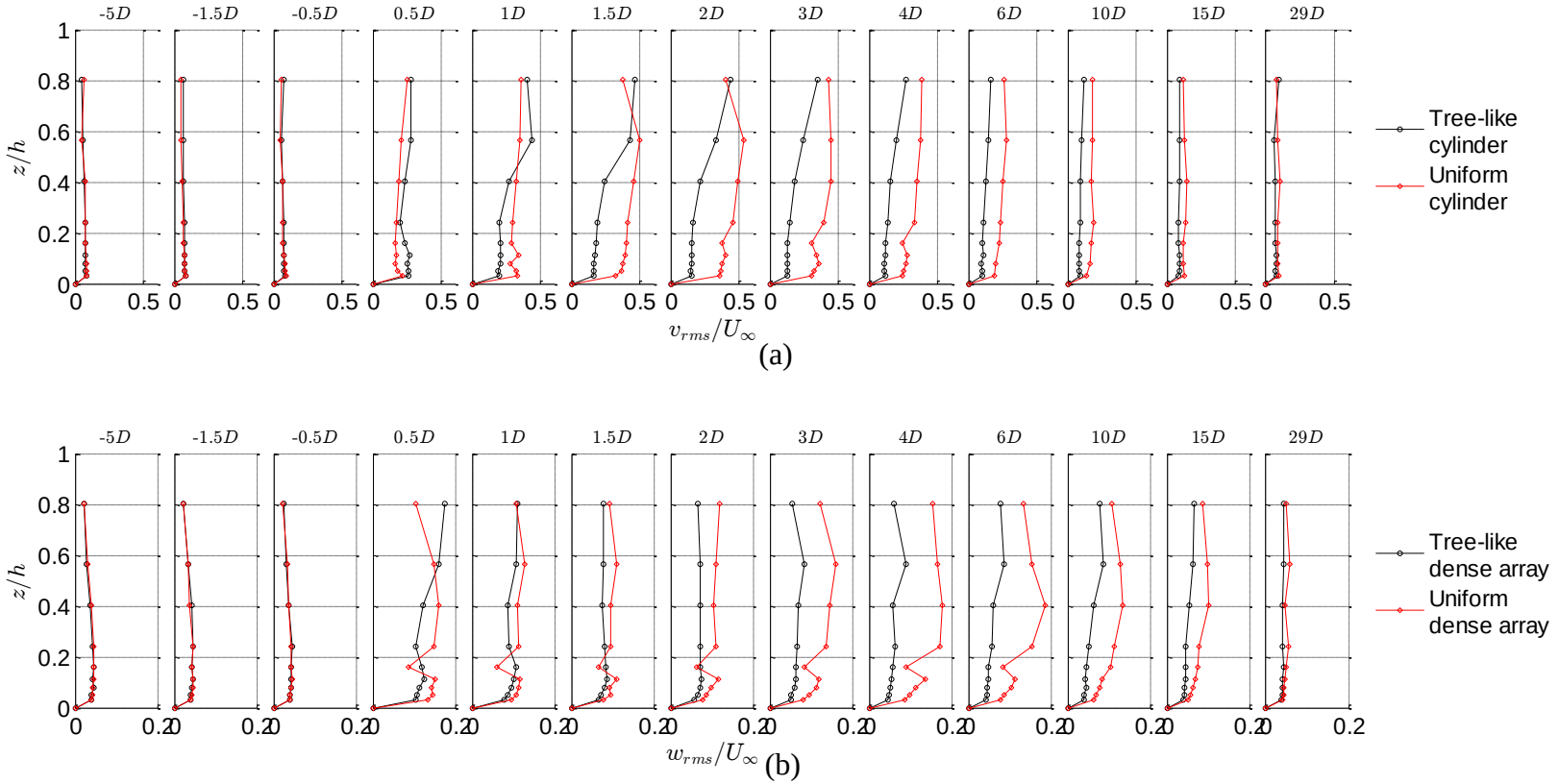

Figure 3.4 : Lateral turbulence intensity v_{rms} profiles for flow over depthwise uniformly shaped emergent obstacle and the corresponding tree-like vegetation where the same obstacle served as the canopy. The obstacle was (a) a solid cylinder and (b) the dense array given in Figure 2.2. The heading of each subfigure denotes the distance from obstacle edge, while the bottom side of the canopy is at $z/h = 0.2$.

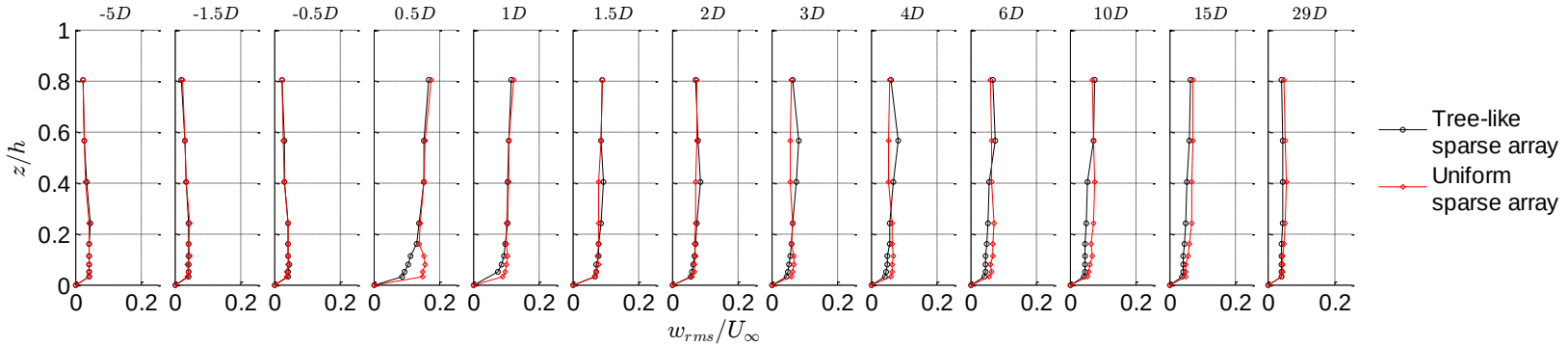

Figure 3.5 : Lateral turbulence intensity v_{rms} profiles for flow over depthwise uniformly shaped emergent obstacle and the corresponding tree-like vegetation where the same obstacle served as the canopy. The obstacle was the sparse array given in Figure 2.2. The heading of each subfigure denotes the distance from obstacle edge, while the bottom side of the canopy is at $z/h = 0.2$.

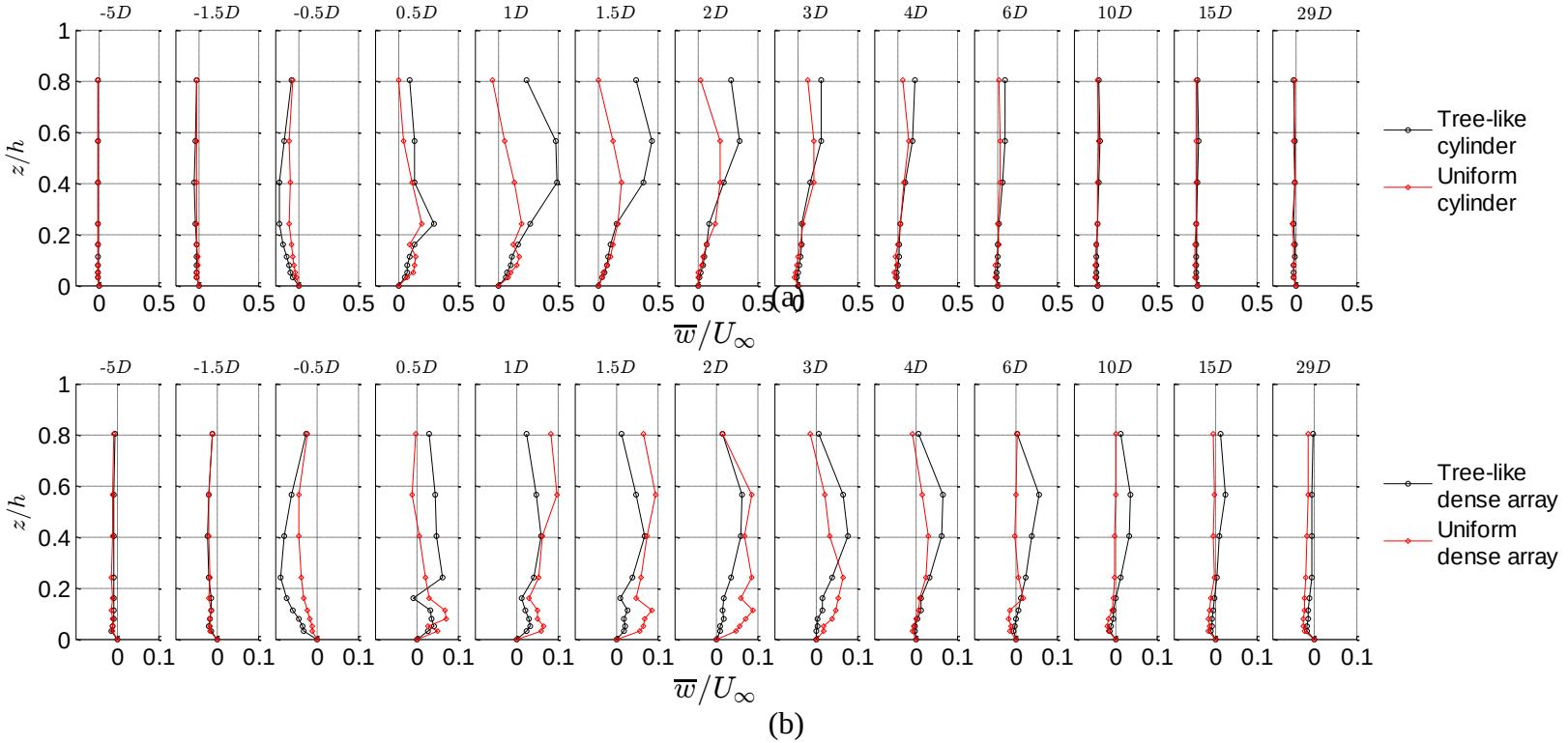

Figure 3.6 : Mean normalized vertical flow velocity $\bar{w}$ profiles for flow over depthwise uniformly shaped emergent obstacle and the corresponding tree-like vegetation where the same obstacle served as the canopy. The obstacle was (a) a solid cylinder, (b) the dense array given in Figure 2.2.The heading of each subfigure denotes the distance from obstacle edge, while the bottom side of the canopy is at $z/h = 0.2$.

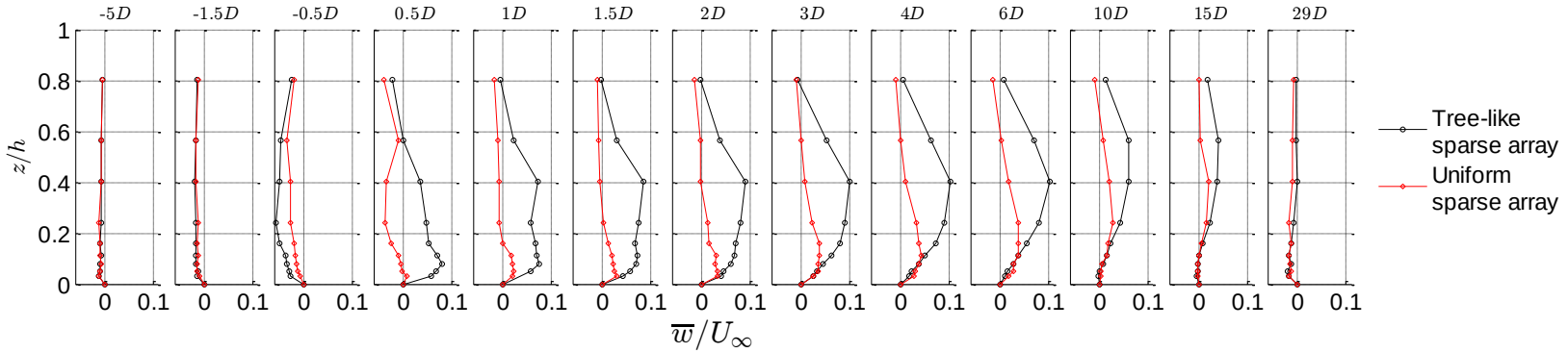

Figure 3.7 : Mean normalized transverse flow velocity $\overline{w}$ profiles for flow over depthwise uniformly shaped emergent obstacle and the corresponding tree-like vegetation where the same obstacle served as the canopy. The obstacle was the sparse array given in Figure 2.2. The heading of each subfigure denotes the distance from obstacle edge, while the bottom side of the canopy is at $z/h = 0.2$.

For tree-like uniform cylinder both subcanopy flow and contracted flow in lateral direction are much stronger then the two other porous objects, thus turbulent mixing and energy transfer between layers are stronger. This leads significantly shorter distance for recovery. Figure 3.8(b) at $-0.5D$ shows how the downflow occurs and gets stronger as the canopy decreases and subsequently enhances the subcanopy flow. Also it is possible to see the vertical energy transfer between layers in Figure 3.8(b) respectively at $0.5D$, $1D$ and $1.5D$. For the tree-like uniform cylinder which disturbs the flow most, the vertical process starts around $z/h = 0.2$ where the interface of trunk and canopy regions and then disperse vertically over distance. The enhanced turbulence mixing with decreasing canopy porosity is evident from Figures 3.9 (a-b), 4.10, which show the increased streamwise, vertical, and transverse turbulence intensity, respectively.

Moreover, Figures 3.9 (a-b), 3.10 show that the near-bed turbulence increases with decreasing canopy porosity and subsequently increasing subcanopy jet intensity. Surprisingly, for the real vegeation even higher projected area than porous tree-like vegetation, turbulence production immediate vicinity downstream the vegetation is significantly lower each longitidunal, lateral and vertical. At least for comparison between real vegetation and sparse tree-like vegetation the bleed flow for sparse condition is higher but turbulence production is also higher, surprisingly. That can be related with the leaf geometry and its turbulence prohibitor characteristic. Also the flexibity of leaf structures is an important feature. It is easy to say the individual turbulence production is lower than the other relevants but for $x > 3D$, the effect of patch scale turbulence can be seen for real vegetation and its effect more distinct relatively, mostly in between $z = 0.2h$ and $z = 0.6h$ where the projected area is higher.

Figure 3.11, 3.12, 3.13, 3.14, 3.15 and 3.16 shows the contour plots of TKE (normalized by U_∞^2) in the horizontal-vertical plane along the flume centerline, combined with the velocity vectors consisting $\bar{u}$ and $\bar{w}$ normalized with U_∞. The contour plot and the depicted vectors are the result of gridded interpolation among the ADV measurement points, while in the white surface in the vegetation proximity no velocity measurements were conducted since the ADV probe would interfere with the vegetation.

As it can be seen in comparison of Figure 3.11 and Figure 3.12, the subcanopy jet in tree like vegetation obstacle with a cylinder canopy reduces the TKE propagation zone, almost all TKE production is confined close to the surface in the canopy wake, while the near-bed turbulence is significantly lower. At the downstream of the obstacle, the shear layer which develops because of the velocity difference between the canopy and trunk region acts as a wall which the layers it separate. The reason behind this behavior is related with the energy propagation direction. The flow velocity at downstream of the vertical shear layer is much higher than the flow velocity at upstream of it. As a result, flow move towards upstream, the separation and vortex occur in through the wake region. Subsequently, generated TKE in steady wake region cannot propagate through downstream because of the imaginary line of shear layer. Due to the porosity difference, there is an obvious strong difference of subcanopy flow which can be seen in Figure 3.11 and Figure 3.13 between solid cylinder and dense array canopies. Increasee in porosity, leads to decrease in the strength of subcanopy flow. But surprisingly, the subcanopy flow seems to diminish the velocity deficit at the rear side of the vegetation, compared to the uniform dense array case in Figure 3.13 and Figure 3.14. In the uniform dense array case there are two distinct TKE peak zones are visible both in Figure 3.14 and in Figure 3.17.

The one closer to the obstacle is linked with individual cylinders turbulence production, then they lose their effect and an apparent decrease follows. After a while an obvious increase in TKE starts, it should be the effect of vortices which are created by two approaching shear layer through the centerline. The second peak further downstream is due to the array induced turbulence where the two shear layer come together and presumably indicates the formation of von Karman vortex street. These two TKE peaks are linked wih steady wake region. Figure 3.13 shows that the subcanopy flow inhibited the formation of the patch scale von Karman vortex street and diminishes the array scale turbulence generation. In Figure 3.15 and 3.16 TKE generation patterns, look similar since the TKE production is attribitued to lee-wake vortices by individual cylinders rather than the entire array.

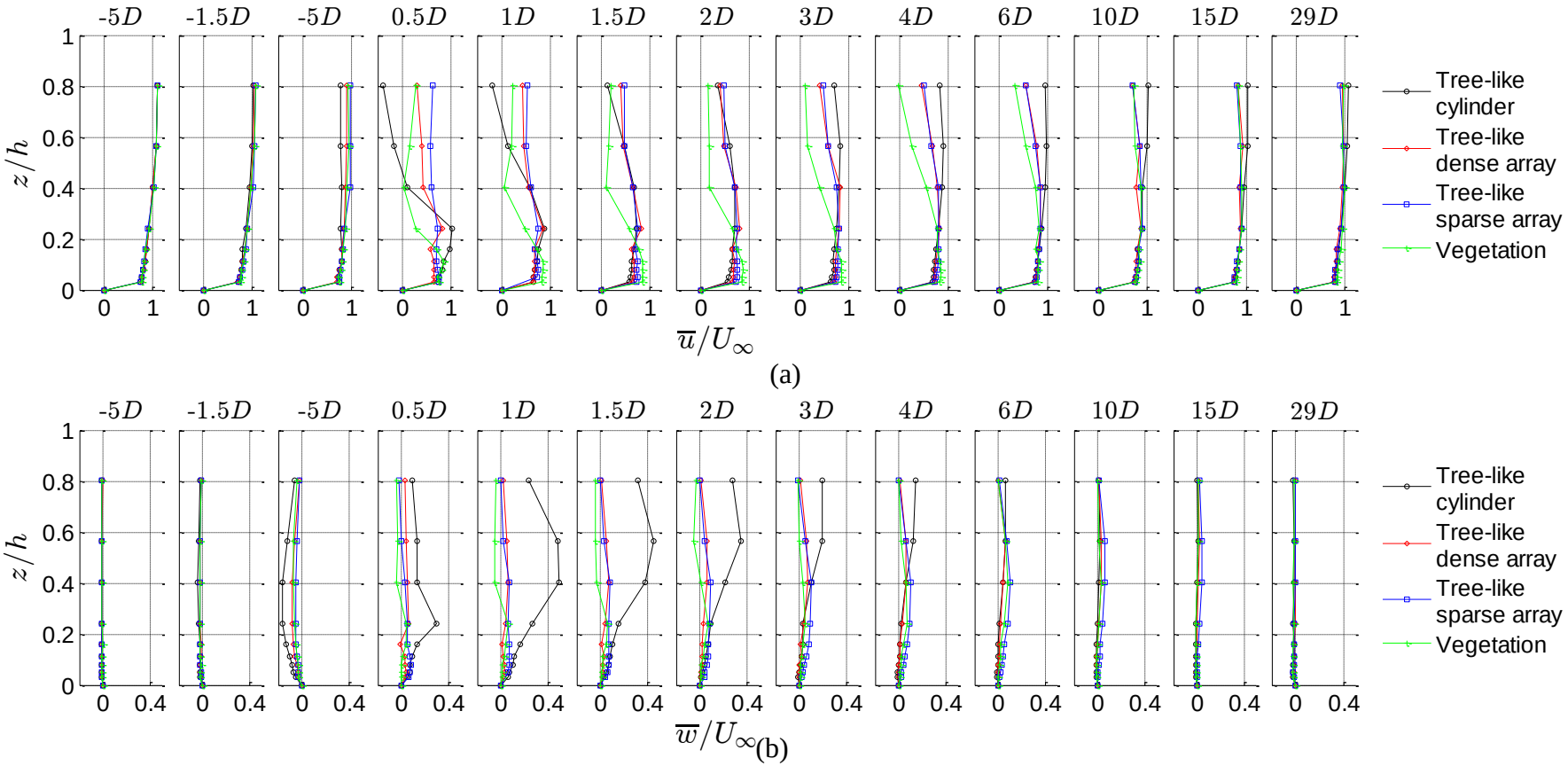

Figure 3.8 : Comperative profiles of the examined tree-like and real vegetal elements for (a) mean streamwise velocity $\bar{u}$, (b) mean vertical velocity $\bar{w}$. The bottom side of canopy is at $z/h = 0.2$.

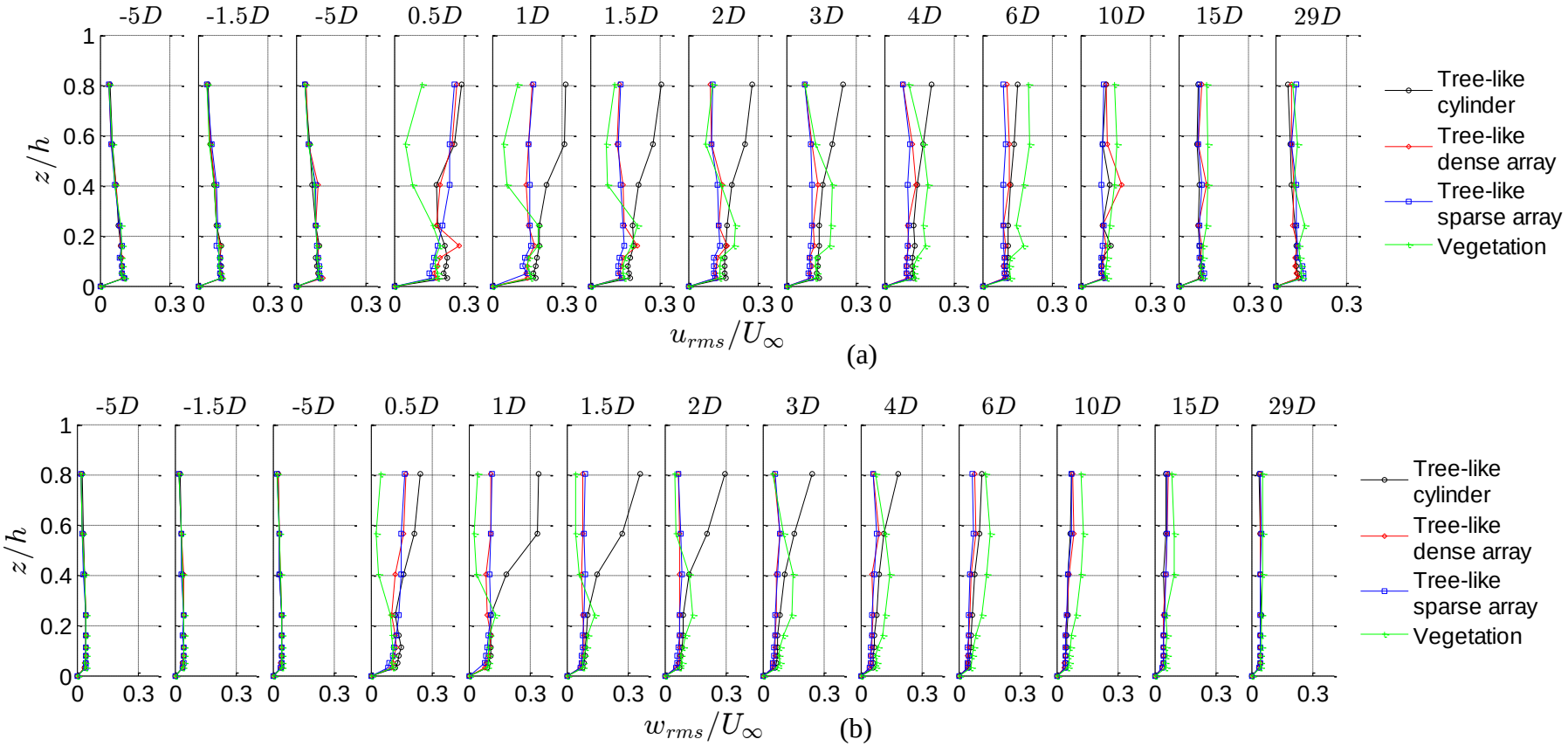

Figure 3.9 : Comperative profiles of the examined tree-like and real vegetal elements for (a) streamwise turbulence intensity u_{rms}, (b) vertical turbulence intensity w_{rms}. The bottom side of canopy is at $z/h = 0.2$.

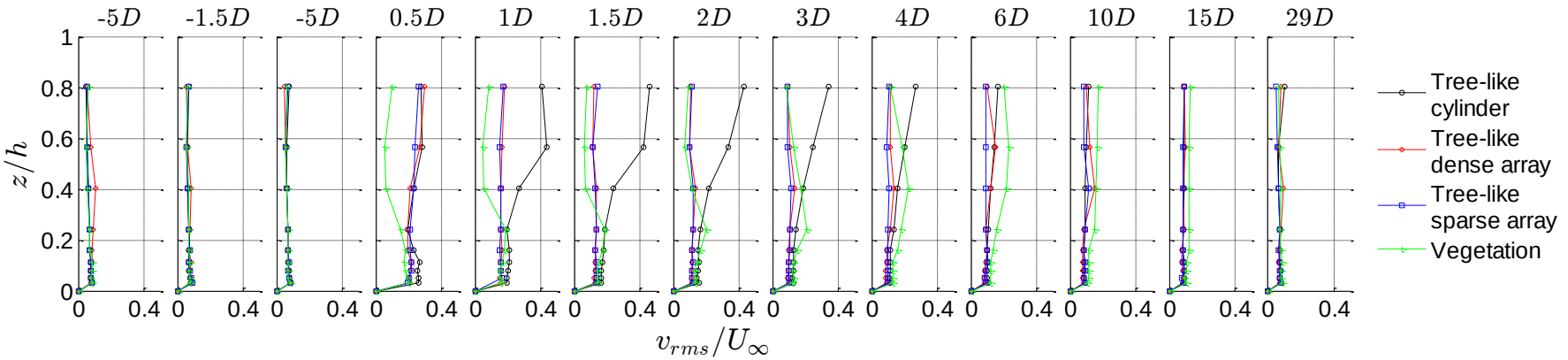

Figure 3.10 : Comperative profile of the examined tree-like and real vegetal elements for streamwise turbulence intensity v_{rms}. The bottom side of canopy is at $z/h = 0.2$.

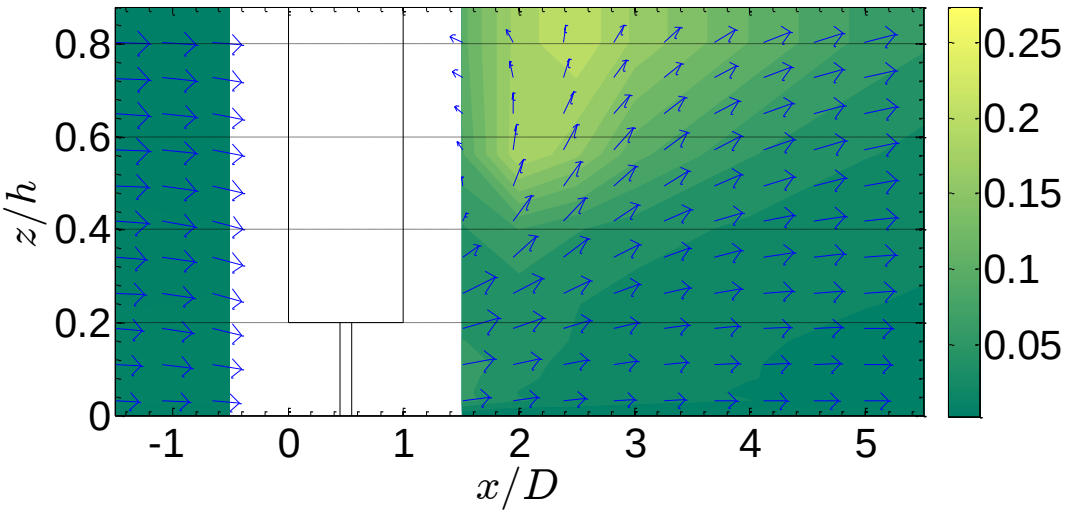

Figure 3.11 : Contour plots of the TKE/U_∞^2 in the horizontal-vertical plane for tree-like vegetation with a cylinder simulating canopy.

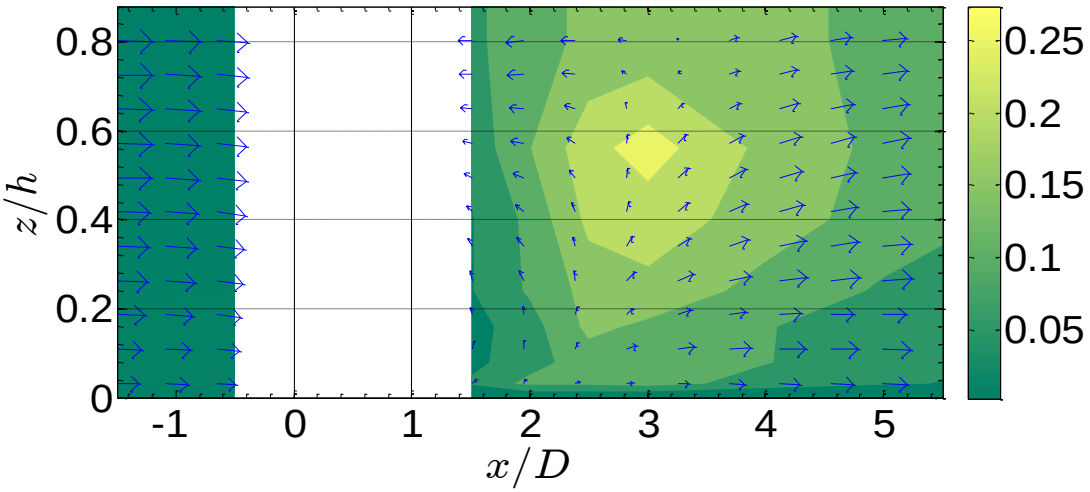

Figure 3.12 : Contour plots of the TKE/U_∞^2 in the horizontal-vertical plane for uniform cylinder vegetation.

Two conclusions can be drawn from this situation. First one is that, the stem scale TKE production occurs in downstream vicinity of individual cylinders and it is not influenced by the subcanopy flow. Two conclusions can be drawn from this situation. First one is that, the stem scale The second one is that, there may not to be a strong subcanopy flow because of the high porosity that can affect the TKE production. In addition, both illations could be valid for this process. Nonetheless, the flow velocity in the bed vicinity behind the tree-like vegetation (Figure 3.15) is significantly increased compared to the uniform sparse array (Figure 3.16) although

downflow and upflow behind the array are weakened compared to dense array configuration.

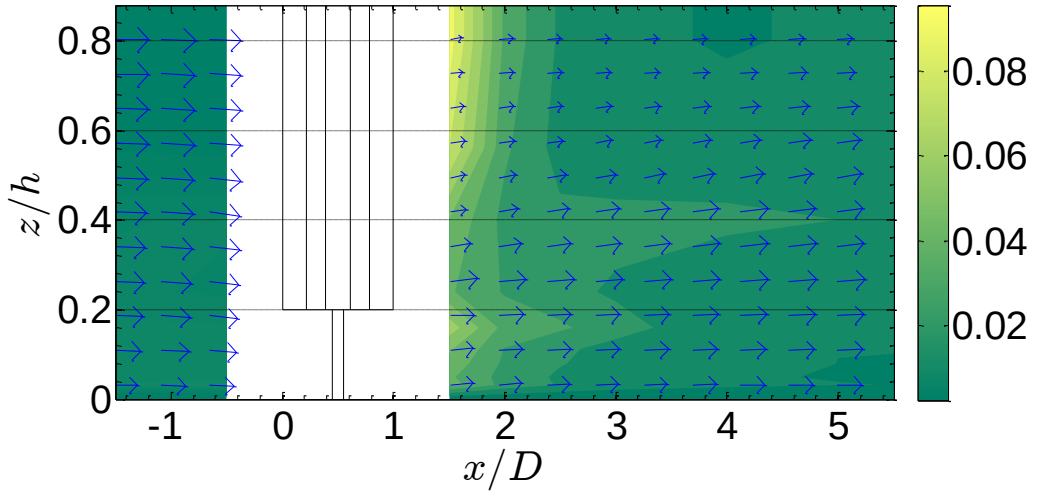

Figure 3.13 : Contour plots of the TKE/U_∞^2 in the horizontal-vertical plane for tree-like vegetation with a tree-like vegetation with a dense cylindrical array simulating canopy.

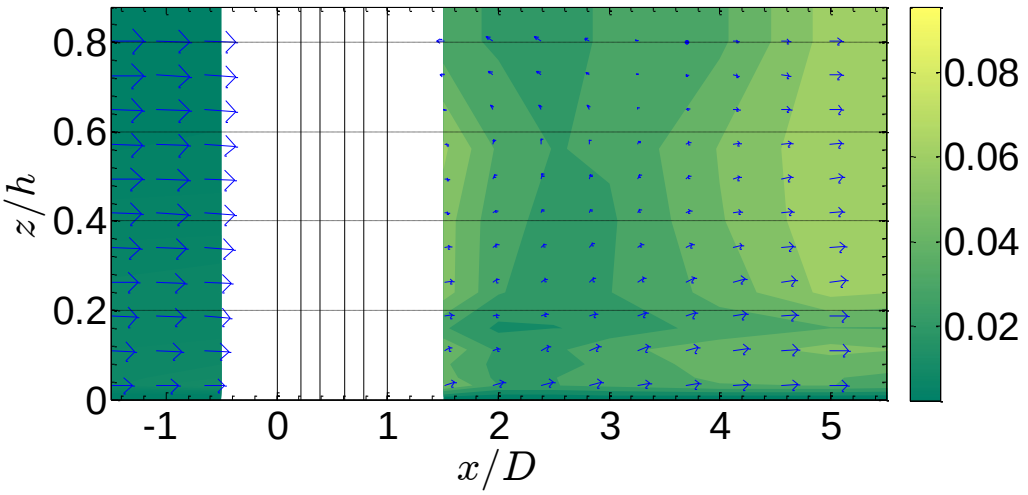

Figure 3.14 : Contour plots of the TKE/U_∞^2 in the horizontal-vertical plane for uniform dense array vegetation.

Figure 3.17 shows the TKE production and $x-z$ plane velocity vectors of real vegetation (*Cupressus mocrocarpa*). The turbulence caused behind the upper part of the vegetation is nearly zero. Also there is not any adverse flow because of the separation. By contrast, with the tree-like solid cylinder, high TKE regions are totally different. Even it can be called transpositioned. In real vegetation condition, the individual structure turbulence can be neglected. We can see there is a bleed flow

because the adverse flow is not that strong as circular cylinder, but the turbulence production is limited. Also, the array scale turbulence production is postponed compared to solid cylinder with the effect of this low turbulenced bleed flow. But the most turbulent section overlaps with the subcanopy jet propagation area, the reason is that the flow velocity difference between the accelerated subcanopy flow and the diminished bleed flow.

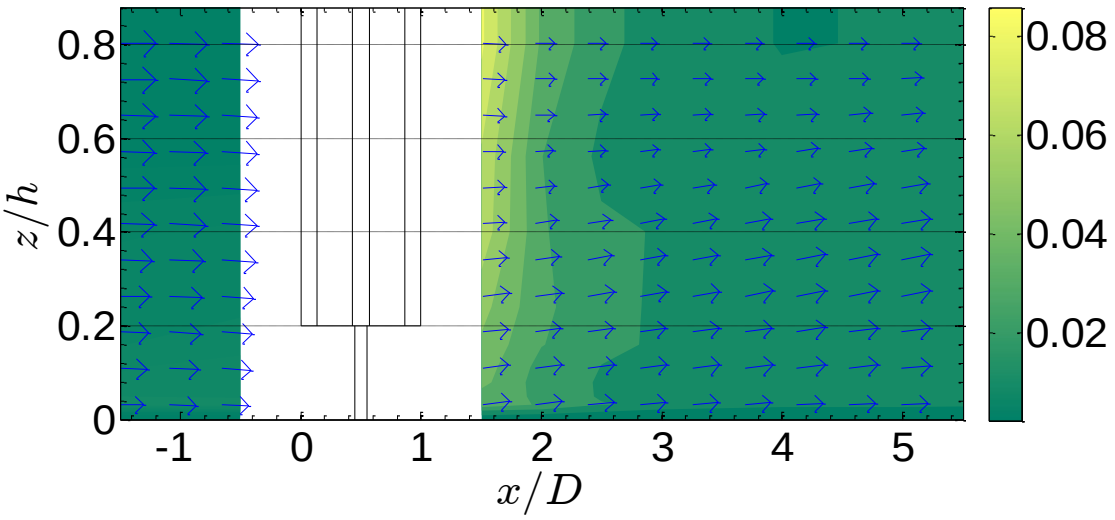

Figure 3.15 : Contour plots of the TKE/U_∞^2 in the horizontal-vertical plane for tree-like vegetation with a tree-like vegetation with a sparse cylindrical array simulating canopy.

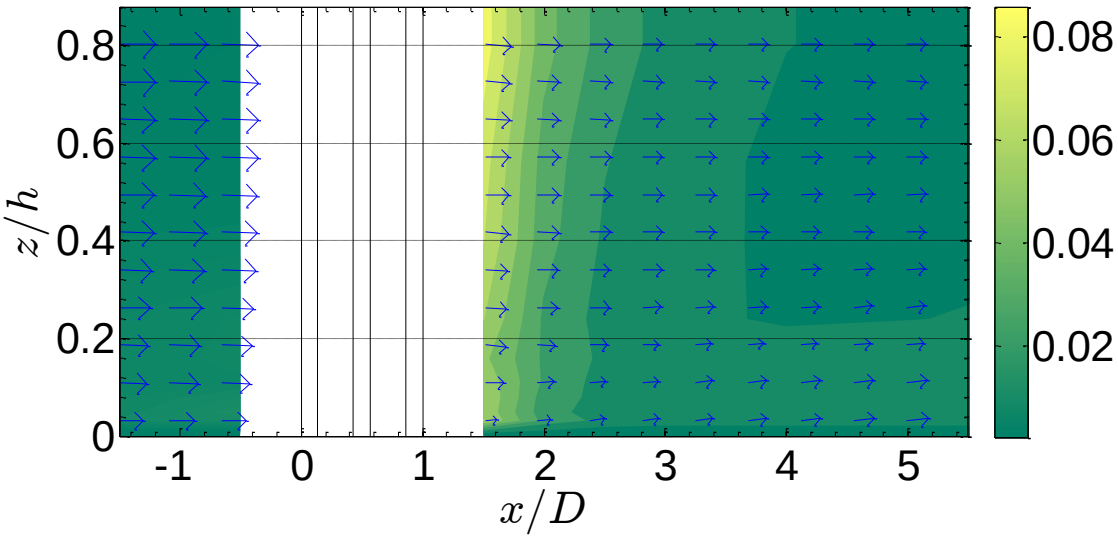

Figure 3.16 : Contour plots of the TKE/U_∞^2 in the horizontal-vertical plane for uniform dense array vegetation.

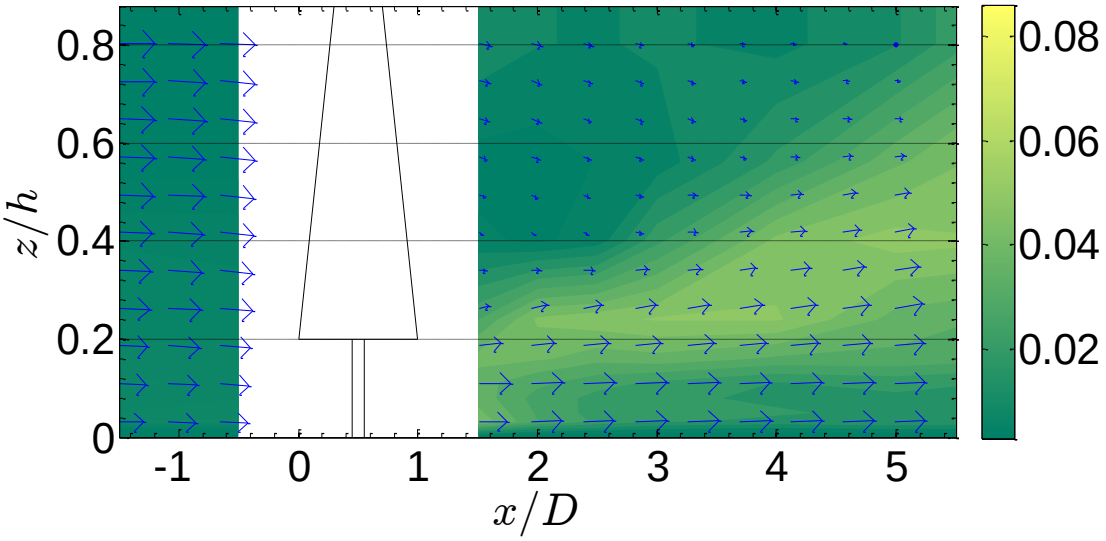

Figure 3.17 : Contour plots of the TKE/U_{∞}^{2} in the horizontal-vertical plane for real vegetation (*Cupressus macrocarpa*).

In comparison with the real vegetation and the tree-like or solid vegetation, a result can be driven as 'any of the representative obstacles reflect the correct real vegetation behavior'. The reason behind it mostly, representative obstacles does not similar to our real vegetation in terms of geometry and leaf structure.

Figures 3.18 and 4.19 shows the variation of depth-averaged normalized mean streamwise flow velocity U and TKE, respectively, along the flume centerline for all studied cases. For the uniform and tree-like forms of solid cylinder flow recovers in shorter distance due to increased velocity deficit and enhanced turbulence, which accelerates mixing Figure 3.18. The flow recovery for the uniform dense array observed in a shorter distance compared to the uniform sparse array. However, this is not the case for three-like vegetation where these two elements exhibit a similar pattern. The velocity drop is always lower for form of tree-like vegetation due to the presence of subcanopy flow.

The pattern of the curves in Figure 3.19 agrees with the aforementioned findings, where the turbulence kinetic energy generation lessens with increased porosity. In addition, there are two distinct TKE peaks in the wake of dense uniform array, which agrees well with the findings of Zong and Nepf (2012) and Chen et al. (2012). The first TKE peak, immediately behind the array attributed to stem scale turbulence production, second peak is correlated with the array scale turbulence production and the patch scale von Karman vortex street. According to Chen et al. (2012), "For low-

blockage patches the first peak in turbulence is greater than the second. As the flow blockage decreases, the second peak moves downstream and decreases in magnitude, indicating that the strength of von Karman vortex street is declining" (p.7). Same TKE reactions observed in this research also.

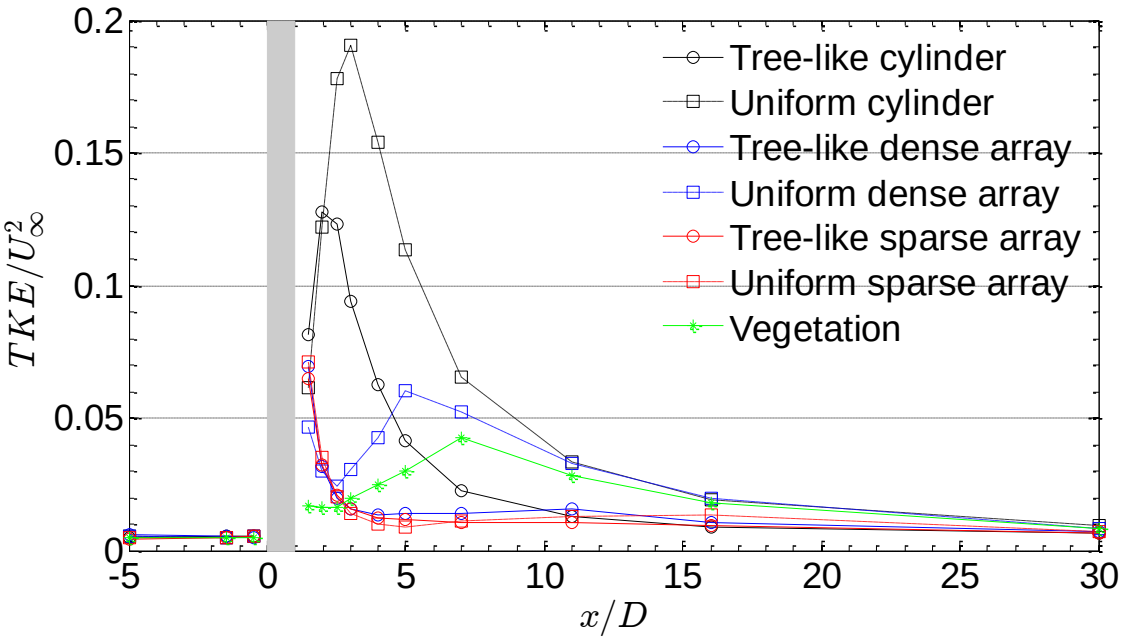

Figure 3.18 : Progression of the mean depth-averaged normalized streamwise TKE along the flume direction. The grey area denotes the position of the vegetal element.

For uniform dense array, second peak is greater than the first, but for uniform sparse array this form changes and first peak becomes greater which represent patch scale TKE production delays and diminishes. The interesting behavior here is, if we compare the first TKE peaks, which represent individual scale TKEproduction, sparse array generates greater turbulence than the dense array (Figure 3.19, Figure 3.21(b) and Figure 3.22(b)). Presumably, because of the subcanopy flow this phenomenon is not observed for the tree-like vegetation cases. It can be seen in both figures that the wake does not fully recover because the momentum deficit due to drag must remain constant downstream of obstacle (Zong & Nepf, 2012).

For uniform vegetation elements the turbulence instensities higher when they compared with respective tree-like elements for all velocity components. This is less obvious for the sparse array, in Figures 3.22, due to the increased porosity.

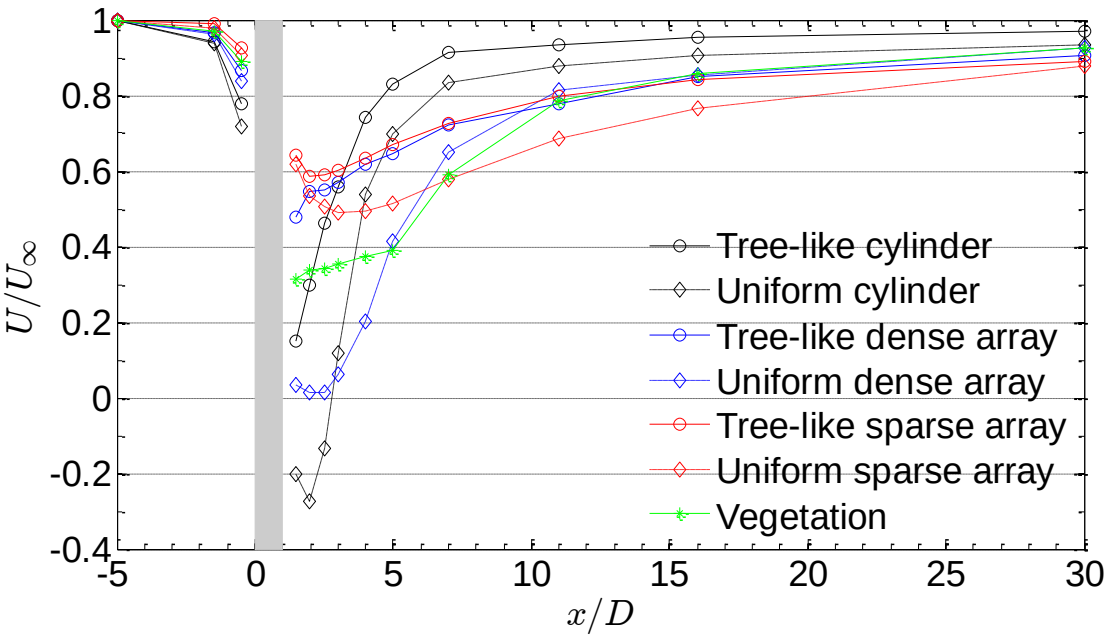

Figure 3.19 : Progression of the mean depth-averaged normalized streamwise flow velocity U along the flume direction. The grey area denotes the position of the vegetal element

Due to flow separation and the strong lateral gradient of the streamwise velocity behind the vegetation, V_{rms} is significantly increased. However with the flow recovery process it attains to similar magnitudes to U_{rms}. W_{rms} is consistently smaller than the other turbulence intensity components in all cases. Two peaks in all turbulence intensities are obvious for the uniform dense array at downstream. Also for the sparse array, this phenomenon is observable. As it mentioned before, first peak originated from the individual cylinders driven turbulence generation, the latter is attributed to the formation of von Karman vortex street. As can be seen in Figure 3.21(b), most of the turbulence of dense array of the tree-like vegetation emanate from array scale turbulence generation. On the contrary, turbulence due to individual elements is more intense than array scale production for sparse array (Figure 3.22). For the tree-like vegetation element, the turbulence intensity peaks are closer to the vegetal element for the permeable canopies cases, compared to the solid cylinder one. It could be an evidence of early formation of von Karman vortex street for tree-like elements compared to uniform elements. For both dense and sparse canopies, a rapid drop of the turbulence intensities observed following the peak. In the consequence of drop, they remain relatively constant until $x/D = 11$ and diminish until the flow recovers.

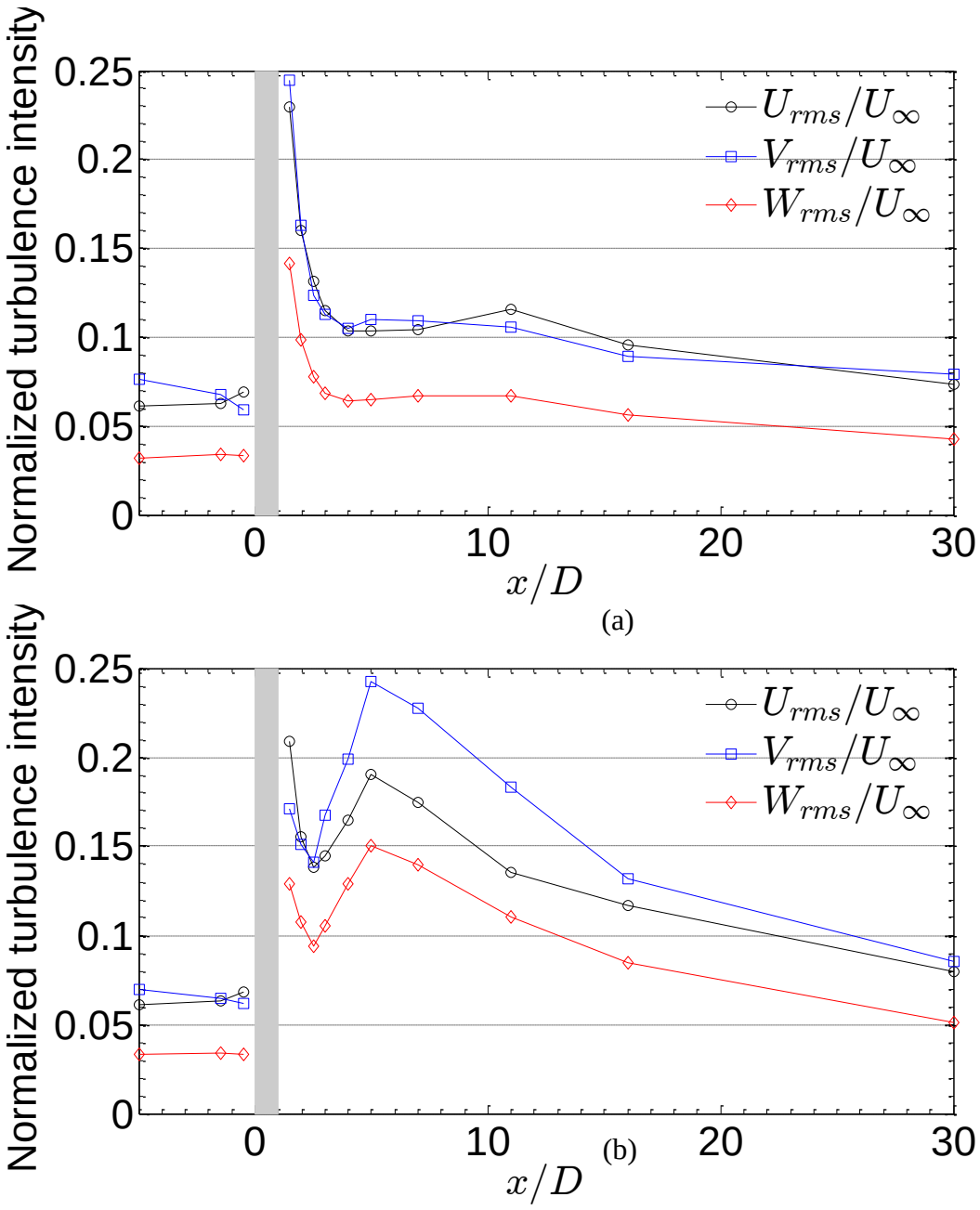

Figure 3.20 : Progression of the normalized depth averaged streamwise U_{rms}, transverse V_{rms} and vertical W_{rms} turbulence intensities for (a) tree-like vegetation with a dense array simulating the canopy (b) uniform dense array vegetation.

Figures 3.21, 3.22 and 3.23 show the progression of the normalized depth-averaged turbulence intensities U_{rms}, V_{rms} and W_{rms} along the flume centerline for all the studied cases.

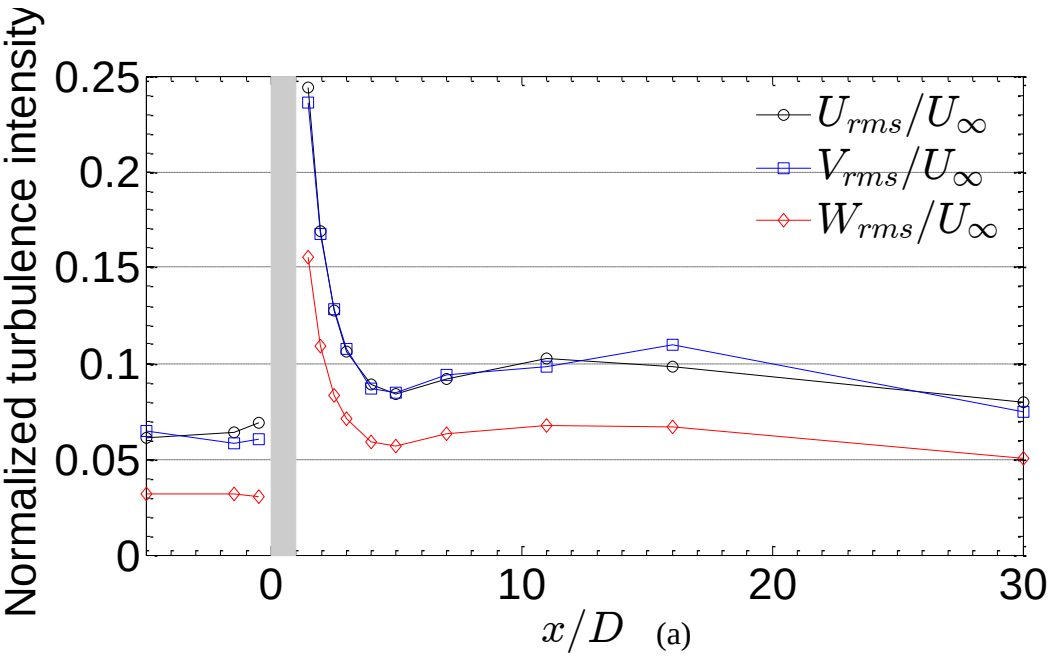

(a)

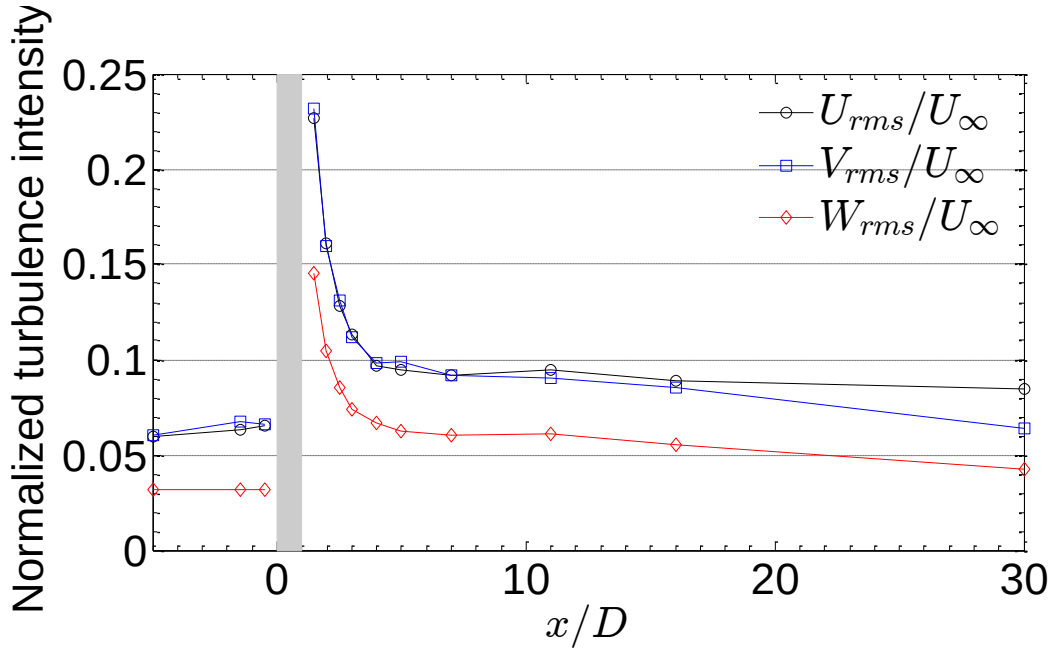

(b)

Figure 3.21 : Progression of the normalized depth averaged streamwise U_{rms}, transverse V_{rms} and vertical W_{rms} turbulence intensities for (a) tree-like vegetation with a sparse array simulating the canopy (b) uniform sparse array vegetation.

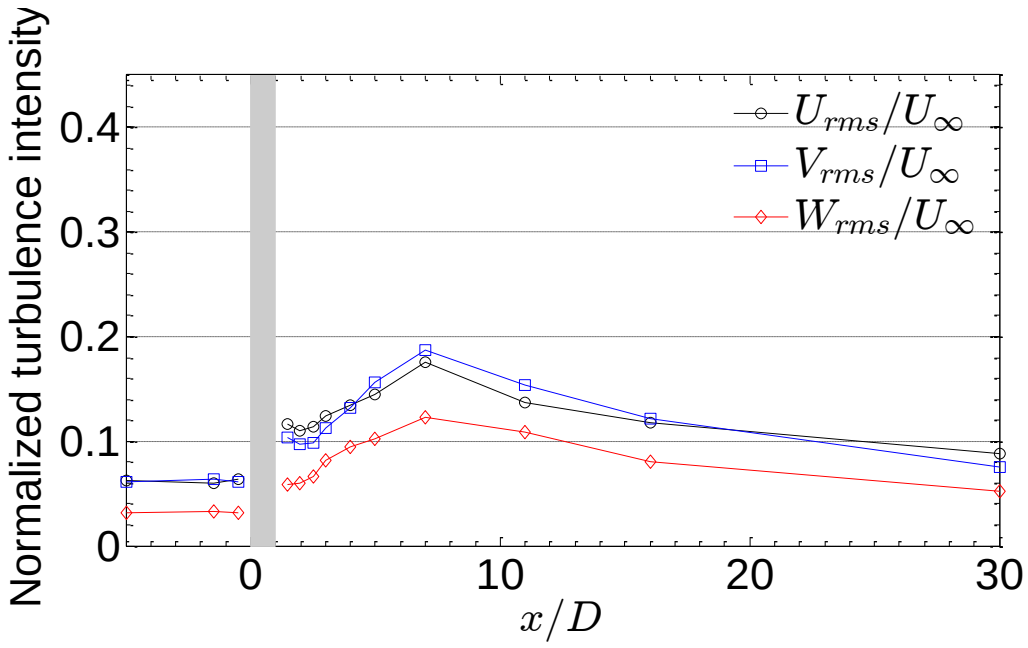

Figure 3.22 : Progression of the normalized depth averaged streamwise U_{rms}, transverse V_{rms} and vertical W_{rms} turbulence intensities for real vegetation

Actually, flow field in proximity of tree-like vegetation consist of two distinct regions across the depth, namely the trunk region and the canopy region. Because the physical processes and behaviours vary for two different region, they also can be investigated separately. Figures 3.23, 3.24, 3.25 show the progression of the normalized $\bar{u}$ and TKE, along flume centerline, at 17.5 cm and 5 cm above the bed, velocity pattern below the canopy for tree-like vegetation. Below the canopy for tree-like vegetation the longitudinal velocity pattern is significantly different for all examined cases compared to the uniform vegetation. In addition, also for the measurements above 17.5 cm above the bed which remain within canopy region, significant differences deduced. For the uniform cylinder compared to tree-like counterpart, the circulation zone behind the obstacle (where streamwise mean velocity is negative) extends to a longer distance. As Zong and Nepf (2012) denoted, a constant streamwise velocity region behind the cylinder observed for uniform dense array, which is linked with steady wake region. Nevertheless, subcanopy flow, which exists in its tree-like counterpart, seems disturbing or diminishing the effect of the steady wake region. As can be seen in Figure 3.23, at 17.5 cm above the bed the tree-like sparse array causes similar pattern of velocity drop but it recovers sharper compared to its unifom counterpart. However, the two TKE peaks are observable at both 5 cm and 17.5 cm in Figures 3.23(a) and 3.24(a) from the bed for uniform dense

array. For tree-like dense array and sparse array this phenomenon is mildly apperent with some alteration as the intensities of first peak and second peak switched. For tree-like sparse array, the two peak of TKE phenomenon is nearly dissepeared.

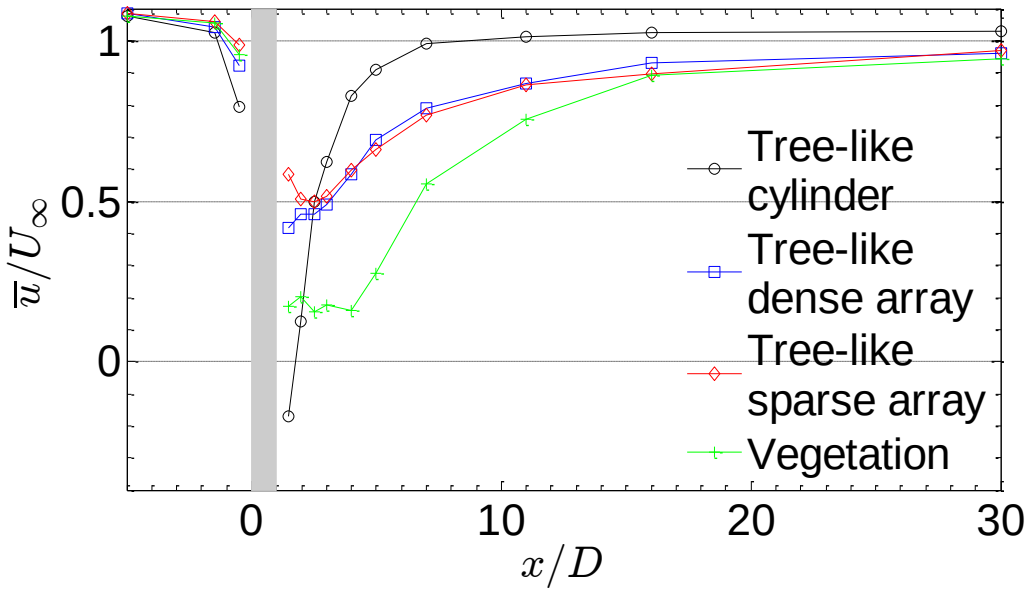

(a)

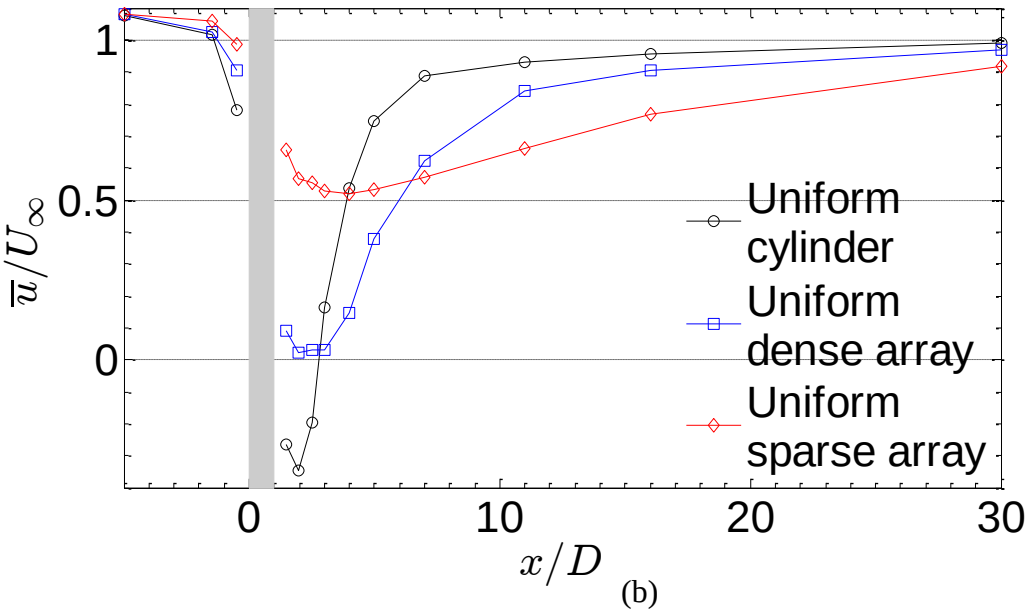

(b)

Figure 3.23 : Progression of the normalized mean streamwise flow velocity along the flume centerline at (a) 17.5cm above the bed for tree-like and real vegetation, (b) 17.5 cm above the bed for uniform vegetation.

This means that, the absence of the peaks is not due to depth averaging of TKE, it is owed to a physical fact that the subcanopy jet distrurbs the flow behind the canopy.

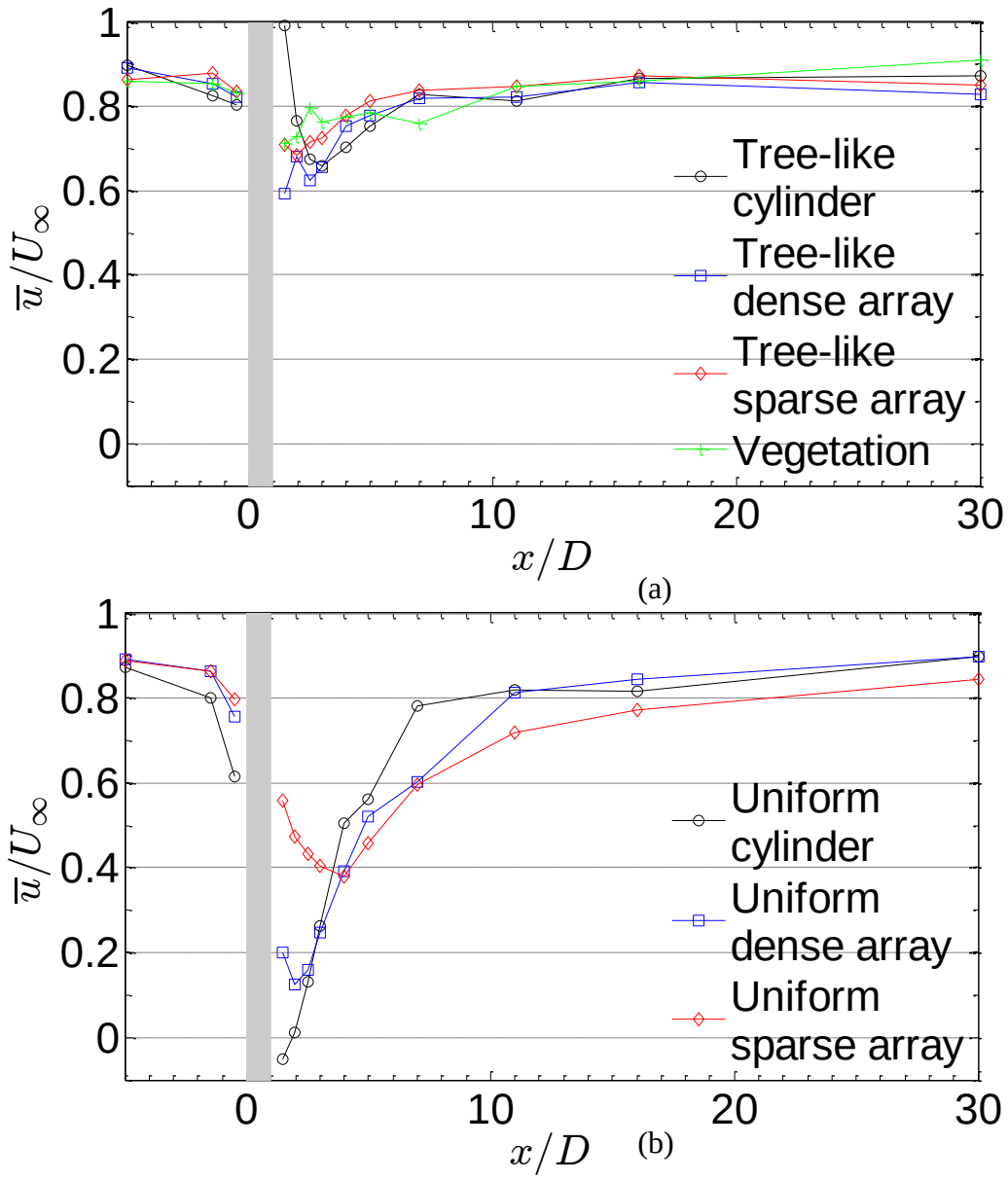

Figure 3.24 : Progression of the normalized mean streamwise flow velocity along the flume centerline at (a) 5cm above the bed for tree-like and real vegetation, (b) 5 cm abover the bed for uniform vegetation.

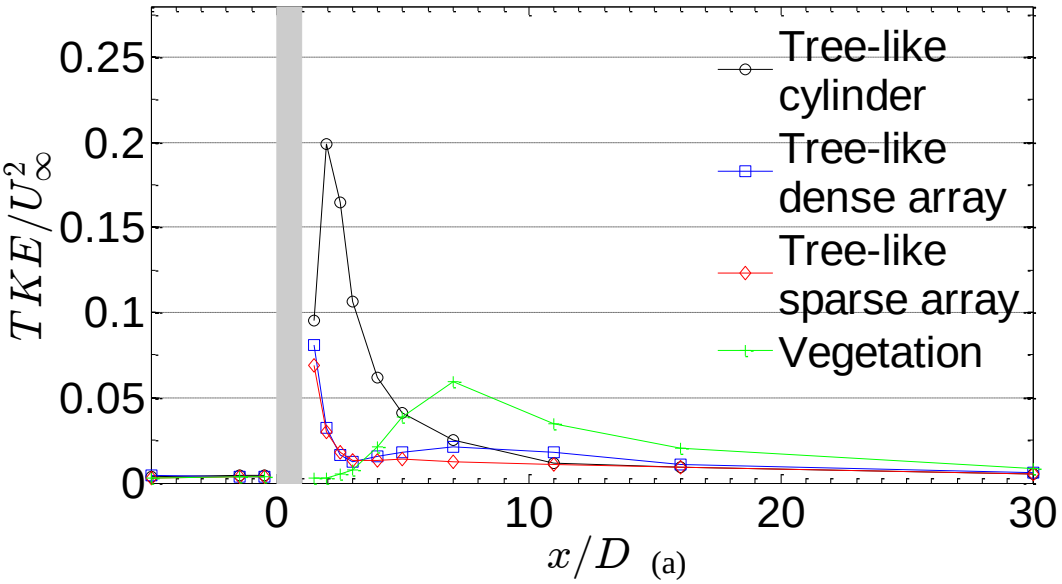

(a)

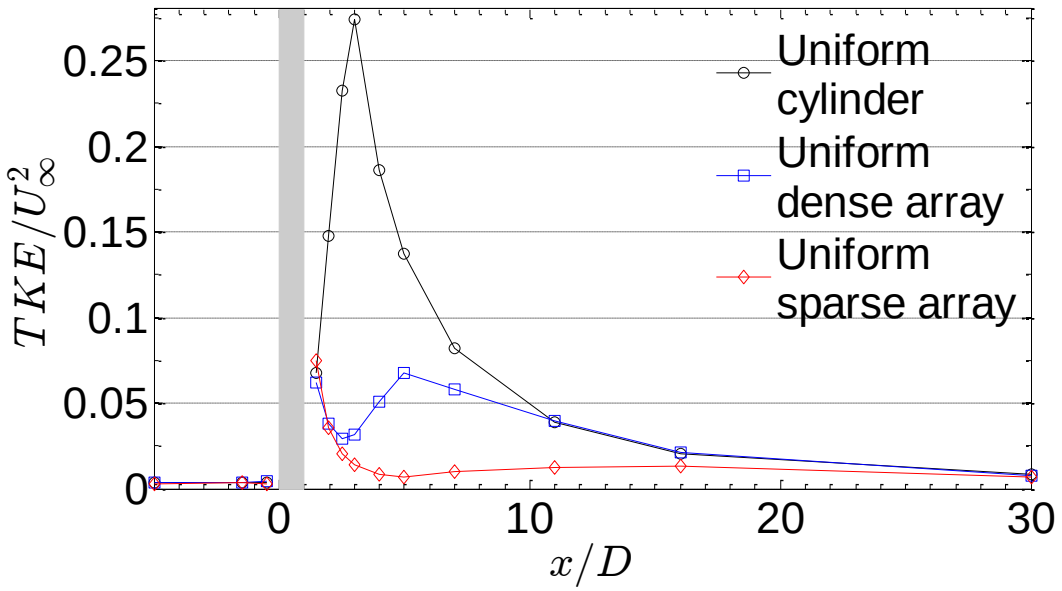

(b)

Figure 3.25: The progression of the normalized turbulence kinetic energy along the flume centerline at 17.5 cm above the bed (a) for tree-like and real vegetation (b) for uniform vegetation.

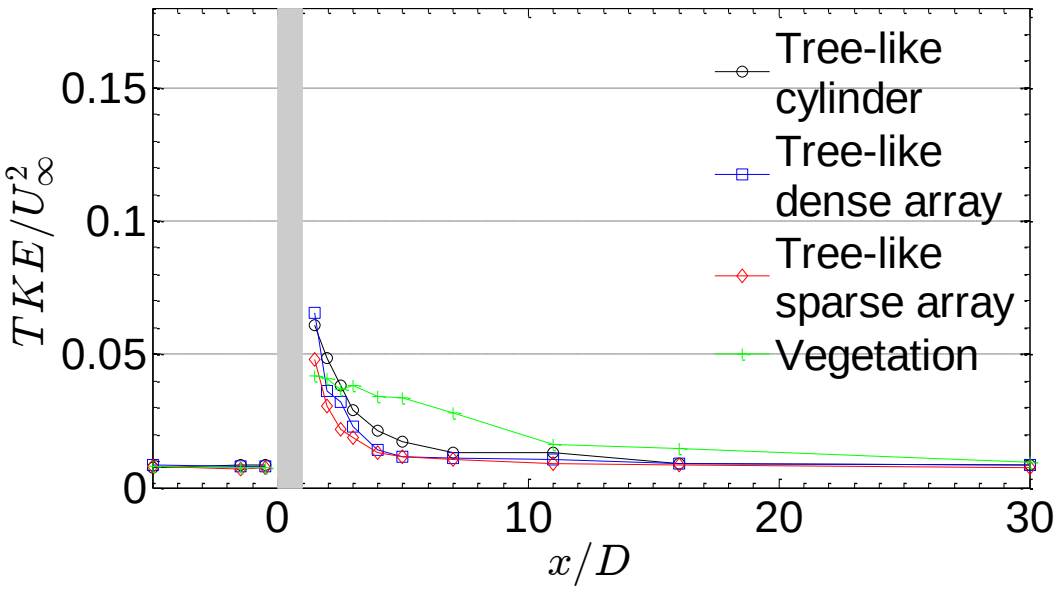

(a)

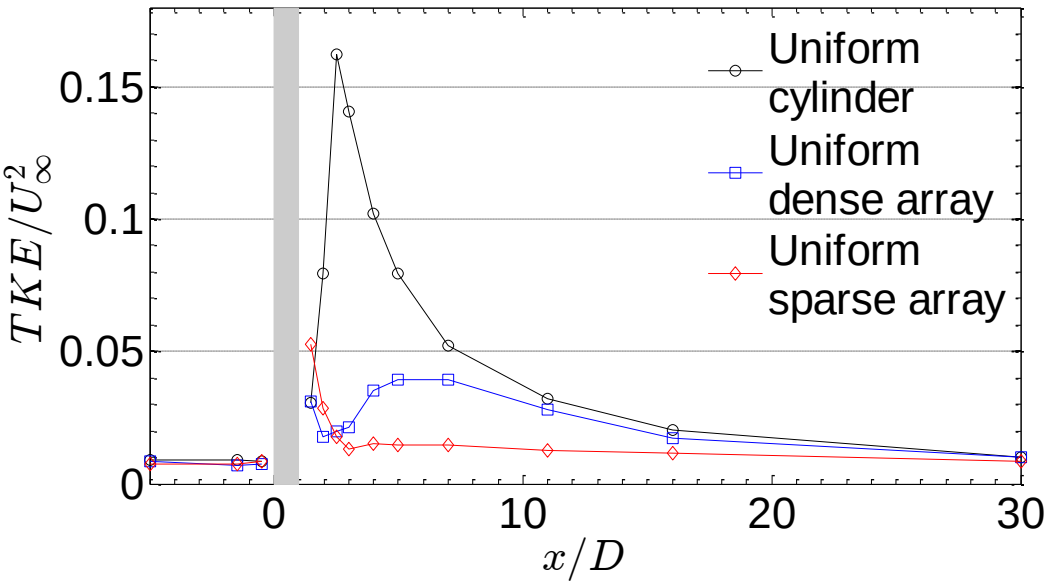

(b)

Figure 3.26: The progression of the normalized turbulence kinetic energy along the flume centerline at 5 cm above the bed (a) for tree-like and real vegetation (b) for uniform vegetation.

4. CONCLUSION AND RECOMMENDATIONS

Implementations such as isolating of the rivers from floodplains through floodwalls, channelization programs, cleaning hydrophytes in order to decrease the river roughness, building dams can given as examples for this kind of river engineering exercises. However, in the last decade a new approach rised called ecological engineering. The reflection of ecological engineering in river engineering comes up to river restoration trend, which refers to the process of supporting the recovery of a damaged or destroyed ecosystem. Applying an ecological, multi-functional and sustainable river restoration requires comprehending deeply the both aquatic and riparian vegetation's role. The motivation for this thesis can summarized as, enhancing comprehension on riparian vegetation's effect to the flow.

The results showed that the existence of the canopy significantly alters the flow field downstream the vegetation. In addition, according to the results simplifying tree-like vegetation with uniform arrays is inadequate to reflect the real affect. The findings of the present study are summarized in the following:

- The wake behind a tree-like structure can be distinguished in two different regions across the depth, which are named trunk region and the canopy region. With the increasing porosity of the canopy, the difference between both regions diminishes.
- With increasing canopy permeability, downflow diminishes due to the increasing intensity of bleed-flow. This results, less distinct downflow.
- The velocity deficit immediate behind the obstacle generates a shear layer that triggers rapid and strong vertical and lateral mixing. This becomes more pronounced with the increasing strength of the subcanopy flow.
- Due to the shear induced turbulence mixing which generated from the interface between canopy and trunk, flow recovery for tree-like vegetation occurred quicker compared to the respective depthwise uniform elements. However, the difference between fully recovery distances are not significantly distinct.

- The depth-averaged turbulence intensities reduced in all directions compared to their uniform counterparts due to the occurrence of the subcanopy jet in tree-like vegetation.
- For the uniform dense array ($\emptyset = 0.335$), depth-averaged TKE exhibits two significant peaks downstream of the obstacle. The first peak is generated due to individual cylinders and the second one is associated with the scale of entire array of cylinders. However, these two TKE peaks are hardly observed in tree-like vegetation elemens, in addition the intensities of the peaks change places.
- The subcanopy jet in tree like vegetation with a cylinder canopy reduces the TKE propagation zone; almost all elevated values of TKE is confined close to the surface in the canopy wake. The shear layer which develops because of the velocity difference between the the canopy and trunk acts as a wall which the layers it separate. Subsequently, generated TKE in steady wake region cannot propagate through downstream because of the imaginary wall of shear layer.

REFERENCES

Aerospaceweb. (2015). *Aerospaceweb.*Retrieved from http://www.aerospaceweb.org http://www.aerospaceweb.org/question/aerodynamics/q2015.shtml

Bennet, S. (2004). Effects of emergent riparian vegetation on spatially averaged and turbulent flow within an experimental channel. In S. Bennet, & A. Simon, *Riparian Vegetation and Fluvial Geomorphology* (pp. 29-41). Washington, DC: American Geophysical Union.

Bennet, S., Pirim, T., & Barkdoll, B. (2002). Using simulated emergent vegetation to alter stream flow direction within a straight experimental channel. *Geomorphology, 44*, 115-126.

Bennet, S., WU, W., Alons, C., & Wang, S. (2008). Modeling fluvial response to in-stream woody vegetation: implications for stream corridor restorasion. *Earth Surface Processes and Landforms, 32*, 890-909.

Braudrick, C., Dietrich , G., Leverich, G., & Sklar, L. (2009). Experimental evidence for the conditions necessary to sustain meandering in coarse-bedded rivers. *Proceedings of the National Academy of Sciences of the United States of America*,106, pp. 16936-16941.

Brierley, G. J., & Fryirs, K. A. (2005). *Geomorphology and River Management.* Singapore: Blackwell Publishing.

Chen, Z., Ortiz, A., Zong, L., & Nepf, H. (2012). The wake structure behind a porous obstruction and its implications for deposition near a finite patch of emergent vegetation. *Water Resources Research, 48*(9), 509-517.

Christensen, P., & Sorensen, J. (1986). Temporal variation of denitrification activity in plant-covered, littoral sediment from Lake Hampen. *Denmark Applied Environmental Microbiology*, 51, 1174-1179.

Dwyer, J., Wallace, D., & Larsen , D. (1997). Value of woody river corridors in leeve protection along the Missouri River in 1993. *Journal of the American Water Recources Association*, 33, 481-489.

Friedman, J. M., Osterkamp, W. R., & Lewis, W. M. (1996). The role of vegetation and bed-level fluctuations in the process of channel narrowing. *Geomophology, 14*, 341-351.

Goring, D., & Nikora, V. (2002). Despiking acoustic Doppler velocimeter data. *Journal of Hydraulic Engineering, 128*(1), 117-126.

Graf, W., & Yulistiyano, B. (1998). Experiments on flow around a cylinder; the velocity and vorticity fields. *Journal of Hydraulic Research, 36*(4), 637-654.

Gran, K., & Paola, C. (2001). Riparian vegetation controls on braided stream dynamics. *Water Resources Research*, 37, 3275-3283.

Gregory, S., Swanson, F., McKee, A. J., & Cummins, K. W. (1991). An ecosystem perspective of riparian zones. *Bioscience*, 41, 540-551.

Gurnell, A. (2014). Plants as River System Engineers. *39*, 4-25.

Gurnell, A. M., Bertouldi, W., & Corenblit, D. (2012). Changing river channels: The roles of hydrological processes, plants and pioneer fluvial landforms in humid temprature, mixed load, gravel bad rivers. *Earth-Science Reviews*.

Jang, C., & Shimizu, Y. (2007). Vegetation effects on the morphological behavior of alluvial channels. *Journal of Hydraulic Research*, 45, 763-772.

Junk, W. (1989). Flood tolerance and tree distribution in central Amazonian floodplains. L. HolmNielsen, I. Nielsen, & H. Balsley içinde, *Tropical forests: botanical dynamics, spectation, and diversity*. (s. 47-64). Orlando, Florida, USA: Academic Press.

Kondolf, G., & Curry, R. (1984). The role of riparian vegetation in channel bank stability: Camel River, California. R. Warner, & K. Hendrix içinde, *California Riparian Systems: Ecology, Conservation, and Management* (s. 124-133). Berkeley, CA: University of California Press.

Kondolf, G., & Curry, R. (1986). Channel erosion along the Camel River, Monterey County, California. *Earth Surface Processes and Landforms, 11*, 307-319.

Li, S., & Millar, R. (2011). A two-dimensional morphodynamic model of gravel-bed river with floodplain vegetation. *Earth Surface Processes and Landforms*, 36, 190-202.

Madej, M., Weaver, W., & Hagans, D. (1994). Analysis of bank erosion on the Merced River, Yosemite valley, Yosemite National-Park,California, USA. *Environmental Management, 18*, 235-250.

McBride, M., Hession, W., Rizzo, D., & Thompson, D. (2007). The influence of riparian vegetation on near-bank turbulence: a flume experiment. *Earth Surface Processes and Landforms, 32*, 2019-2037.

Mori, N., Suzuki, T., & Kakuno, S. (2007). Noise of acoustic doppler velocimeter data in bubly flows. *Journal of Engineering Mechanics, 133*(1), 122-125.

Munson, B. R., Young, D. F., Okiishi, T. H., & Huebsch, W. W. (2009). *Fundamentals of Fluid Mechanics.* Hoboken,NJ: Wiley & Sons.

Naiman, R. J., & Decamps, H. (1990). *The ecology and management of aquatic-terrestrial ecotones.* Paris, France: UNESCO.

Naiman, R., Decamps, H., Pastor, J., & Johnston, C. (1988). The potential importance of boundaries to fluvial ecosystems. *Journal of the North American Benthological Society*, 7, 289-306.

Nicolle, A., & Eames, I. (2011). Numerical study of flow through and around a circular array of cylinders. *Journal of Fluid Mechanics, 679*, 1-31.

Nielsen, L., Christiensen, P., Revsbech, N., & Sorensen, J. (1990). Denitrification and photosynthesis in stream sediment studied with microsensor and whole-core techniques. *Limnology and Oceanography*, 35, 1135-1144.

Nilsson, C. (1992). Conservation management of riparian communities. L. Hansson içinde, *Ecological principles of nature conservation* (s. 352-372). London, England: Elsevier Applied Science.

Petts, G. (1996). Sustaining the ecological integrity of large floodplain rivers. M. Anderson, D. Walling , & P. Bates içinde, *Floodplain Processes* (s. 535-551). Chichester, UK: Wiley & Sons Ltd.

Raedeke, K. (1989). *Streamside management: riparian wildlife and forestry interactions. Contribution number:59.* (K. Raedeke, Ed.) Seattle, Washington, USA: Institute of Forest Resources.

RESTORE. (2013). *Rivers by Design.* Bristol: Environment Agency.

Roulund, A., Sumer, B., Fredsoe, J., & Michelsen, J. (2005). Numerical and experimental investigation of flow and scour around a circular pipe. *Journal of Fluid Mechanics, 534*, 351-401.

Schulz, M., Kozerski, H. P., Pluntke, T., & Rinke, K. (2003). The influence of macrpohytes on sedimentation and nutrient retention in the Lower River Spree (Germany). *Water Research*, 37, 569-578.

Shields, F., & Gray, D. (1992). Effects of woody vegetation on sandy leeve integrity. *Water Resources Bulletin*, 28, 917-931.

Simon, A., & Hupp, C. (1990). The recovery of alluvial systems in response to imposed channel modifications, West Tennessee, USA. In J. B. Thornes, *Vegetation and Erosion: Processes and Environments.* New York: John Wiley & Sons.

Sumer, B., Christiansen, N., & Fredsoe, J. (1997). The horseshoe vortex and vortex shedding around a vertical wall-mounted cylinder exposed to waves. *Journal of Fluid Mechanics, 332*, 41-70.

Sumer, M. B., & Fredsoe, J. (2006). *Hydrodynamics Around Cylindrical Structures.* Singapore: World Scientific Publishing Co. Pte. Ltd.

Sündback, K., & Miles, A. (2002). Role of microphytobenthos and denitrification for nutrient turnover in embaynments with floating macroalgal mats: a spring situation. *Aquatic Microbial Ecology*, 30, 91-101.

Svendsen, L., Kronvag, B., Laubel, A., Larsen, S., & Andersen, B. (1998). Phosphorus retention in a Danish lowland river system. *Verh Int Verein Limnol*, 26, 956-962.

Tabacchi,, E., Planty-Tabacchi, A., & Decamps, A. (1990). Continuity and discontinuity of the riparian vegetation along a fluvial corridor. *Landscape Ecology*, 5, 9-20.

Takemura, T., & Tanaka, N. (2007). Flow structures and drag characteristics of a colony-type emergent roughness model mounted on a flat plate in uniform flow. *Fluid Dynamics Research, 39*(9-10), 694-710.

Tal, M., & Paola, C. (2007). Dynamic single-thread channels maintained by the interaction of flow and vegetation. *Geology*, 35, 347-350.

Tal, M., Gran, K., Murray, A., Paola, C., & Hicks, D. (2004). Riparian vegetation as a primary control on channel characteristics in multi-thread rivers. In S. Bennet, & A. Simon (Ed.), *Water Science and Application* (Vol. Riparian Vegetation and Fluvial Geomorphology, pp. 43-58). Washington, DC: American Geophysical Union.

Tanaka, N., & Yagisawa, J. (2010). Flow structures and sedimentation characteristics around clump-type vegetation. *Journal of Hydro-Environment Research, 4*(1), 15-25.

Unger, J., & Hager, W. (2007). Down-flow and horseshoe vortex characteristics of sediment embedded bridge piers. *Experimental Fluids, 42*(1), 1-19.

Valyrakis, M., Kitsikoudis, V., Yagci, O., Kirca, V., & Koursari, E. (2015). Experimental investigation of the modification of the flow field, past emergent aquatic vegetation elements. *36th IAHR Congress.* The Hauge, Netherlands.

Wahl, T. (2003). Discussion of "Despiking acoustic doppler velocimeter data". *Journal of Hydraulic Engineering, 129*(6), 484-487.

White, F. M. (2001). *Fluid Mechanics.* Boston: McGraw-Hill.

Williams, P. B. (2001). River Engineering versus River Restoration. *River Restoration Conference.* Nevada: Philip Williams & Associates Ltd.

Yagci, O., Tscheische, U., & Kabdasli, M. (2010). The role of differnet forms of natural riparian vegetation on turbulence and kinetic energy characteristics. *Advances in Water Resources,33(5), 601-614.*

Zong, L., & Nepf, H. (2012). Vortex development behind a finite porous obstruction in a channel. *Journal of Fluid Mechanics, 691*, 368-391.

CURRICULUM VITAE

Name Surname: Dorukhan Kellecioğlu

Place and Date of Birth: Alanya/ANTALYA 02.11.1991

E-Mail: dorukhankellecioglu@gmail.com

EDUCATION:

B.Sc.: Istanbul Technical University / Civil Engineering

M.Sc.: Istanbul Technical University – Hydraulics and Water Resources Programme

OTHER PUBLICATIONS, PRESENTATIONS AND PATENTS :

- Aksoy H., Kirca V.S.O, Bugan H.I., **Kellecioglu D.,** 2015: Determination of Flood-Prone Areas by Soil Wetness Index in River Basins. *National Congress- VIII. National Hydrology Congress,* October 8-10, 2015 Sanliurfa, Turkey
- Burgan H.I., **Kellecioglu D.,** Aksoy H., Kirca V.S.O., 2015: Hydraulic Flood Model Supported with Geographic Information Systems. *National Congress – 4.Hydraulic Structures Symposium,* November 19-21, 2015 Antalya, Turkey